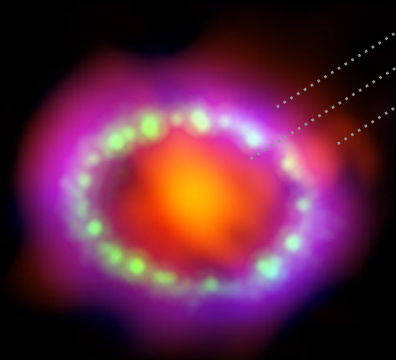


Light at the end of the tunnel: Astrophysical searches for axion-like particles in gamma-ray energies



SN1987A*

NPAC Seminar
UW-Madison Department of Physics
September 8, 2022

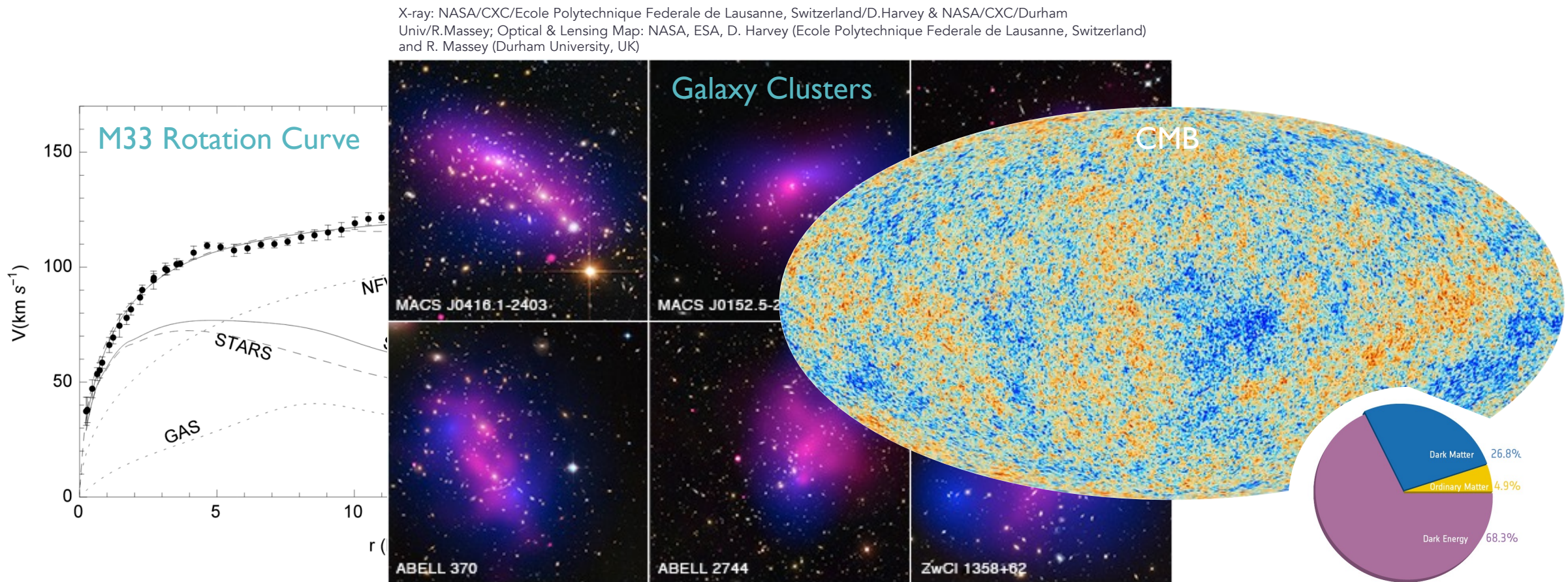
Milena Crnogorčević
University of Maryland/NASA Goddard
mcrnogor@umd.edu

TALK OUTLINE

- Axion-like particles: Introduction and motivation
 - 1. *Fermi-LAT* Low Energy Technique: Sensitivity study
 - 2. Sensitivity of the future MeV instruments
 - 3. Gamma-ray Bursts as ALP factories: what has *Fermi* seen so far?
 - 4. *Fermi-LAT* GRB pre-cursor analysis
- Conclusions & future work

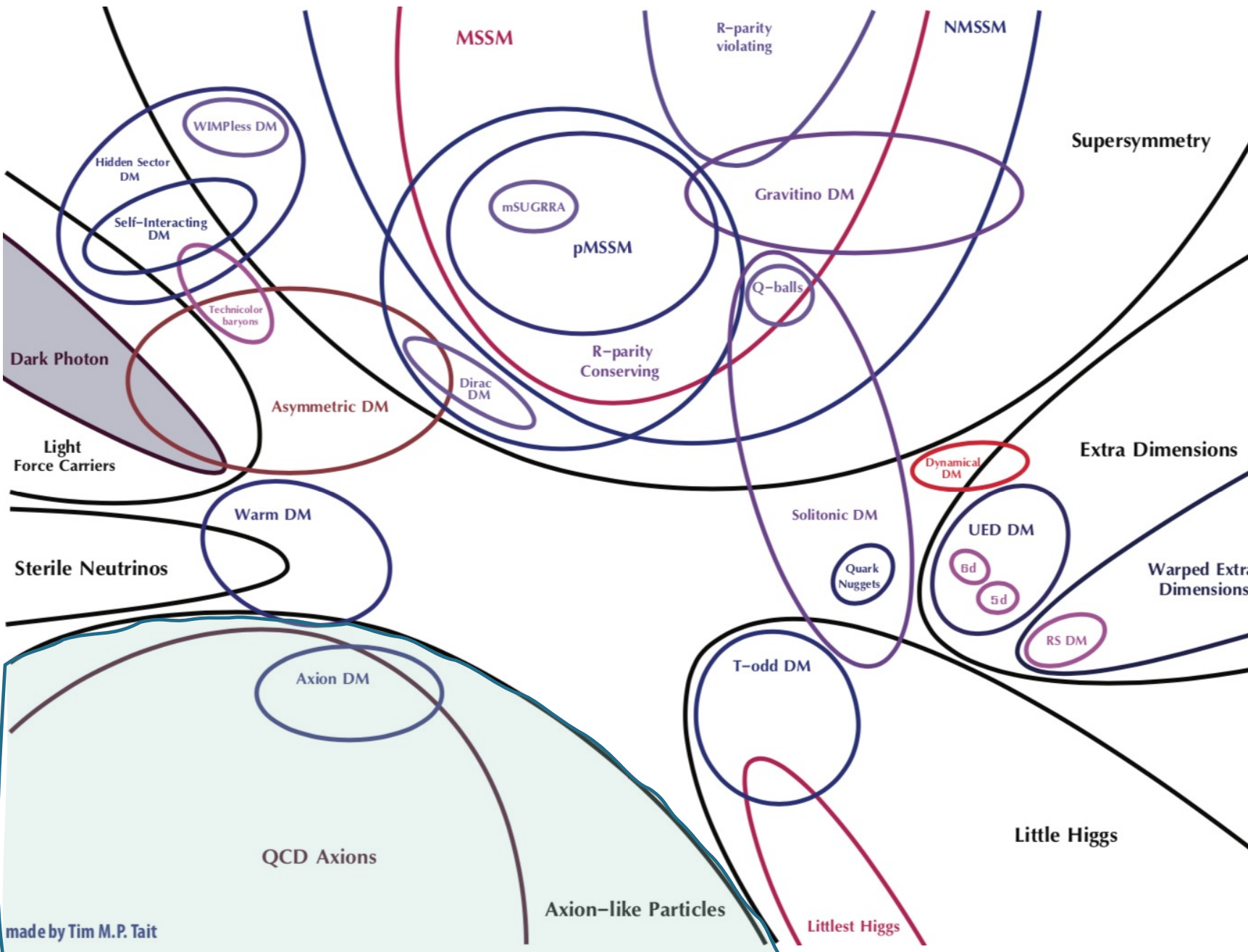
INTRODUCTION AND MOTIVATION

OVERWHELMING EVIDENCE FOR THE EXISTENCE OF DARK MATTER



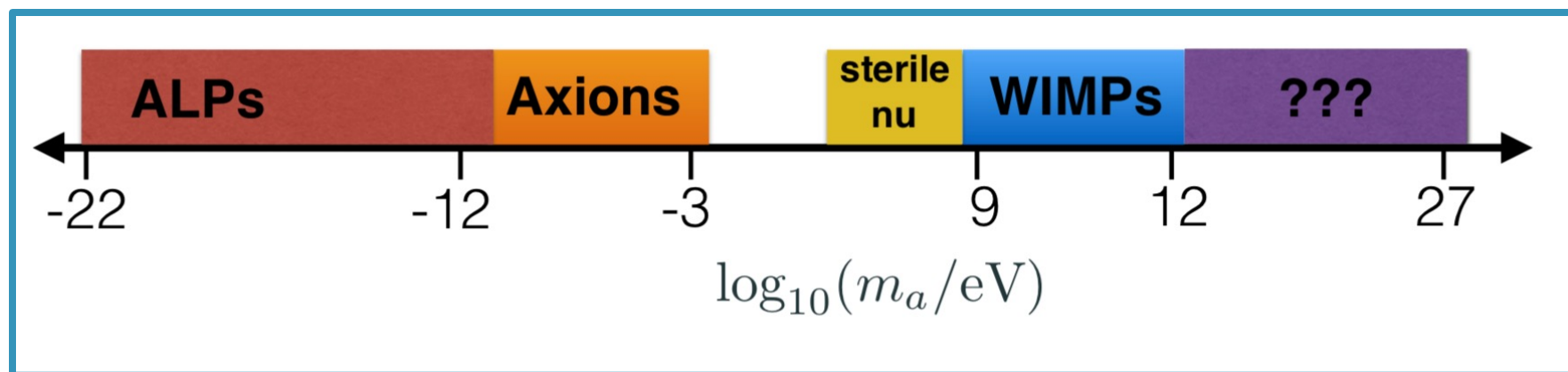
European Space Agency and Planck Collaboration

THE PARTICLE NATURE OF DARK MATTER



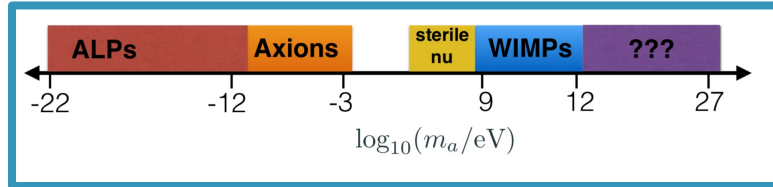
WHAT ARE AXION-LIKE PARTICLES? (ALPs)

- ❖ Extension of the axion, a proposed solution of the strong charge-parity problem in QCD
- ❖ WISPs: weakly-interacting sub-eV particles (mass $\lesssim 10^{-10}$ eV)

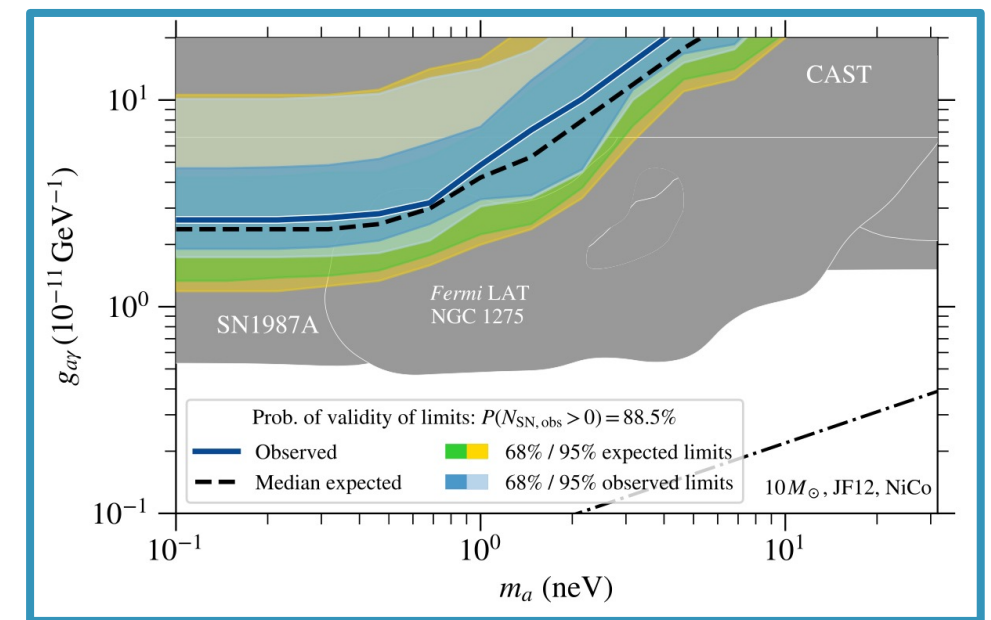


WHAT ARE AXION-LIKE PARTICLES? (ALPs)

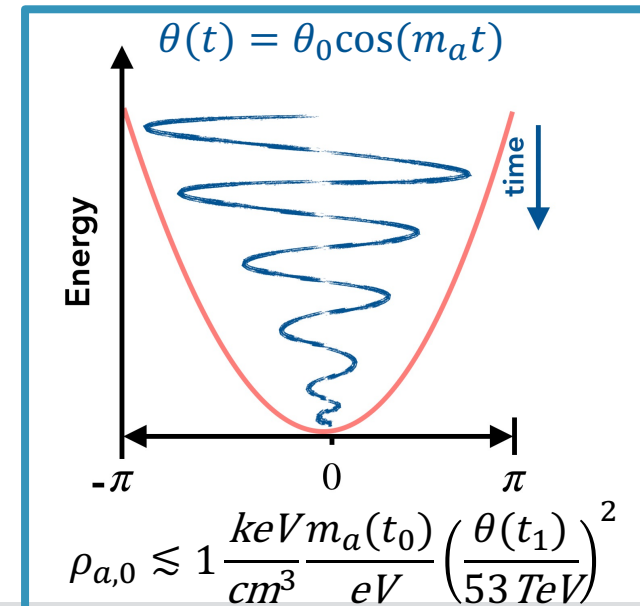
- Extension of the axion, a proposed solution of the strong charge-parity problem in QCD
- WISPs: weakly-interacting sub-eV particles (mass $\lesssim 10^{-10}$ eV)



- Cold matter requirements:
 - ✓ feeble interactions with standard model particles
 - ✓ cosmological stability
- Direct and indirect searches \rightarrow limits on coupling/mass parameter space
- Non-thermal production of ALPs via *misalignment mechanism* or inverse Primakoff process



Exclusion plot for ALPs. [Meyer & Petrushevska 2020]



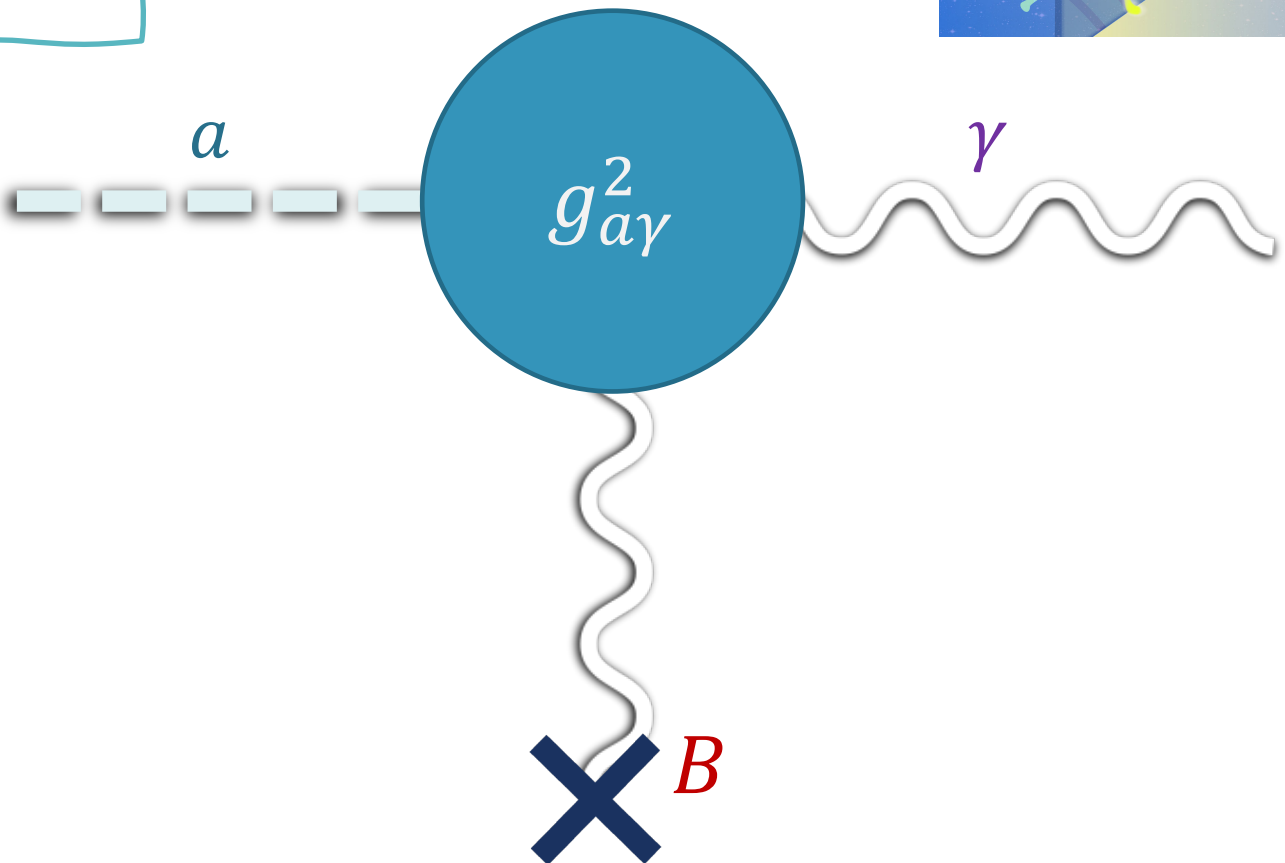
OBSERVING ALPs WITH GAMMA-RAYS

- Primakoff process: converting ALPs into photons

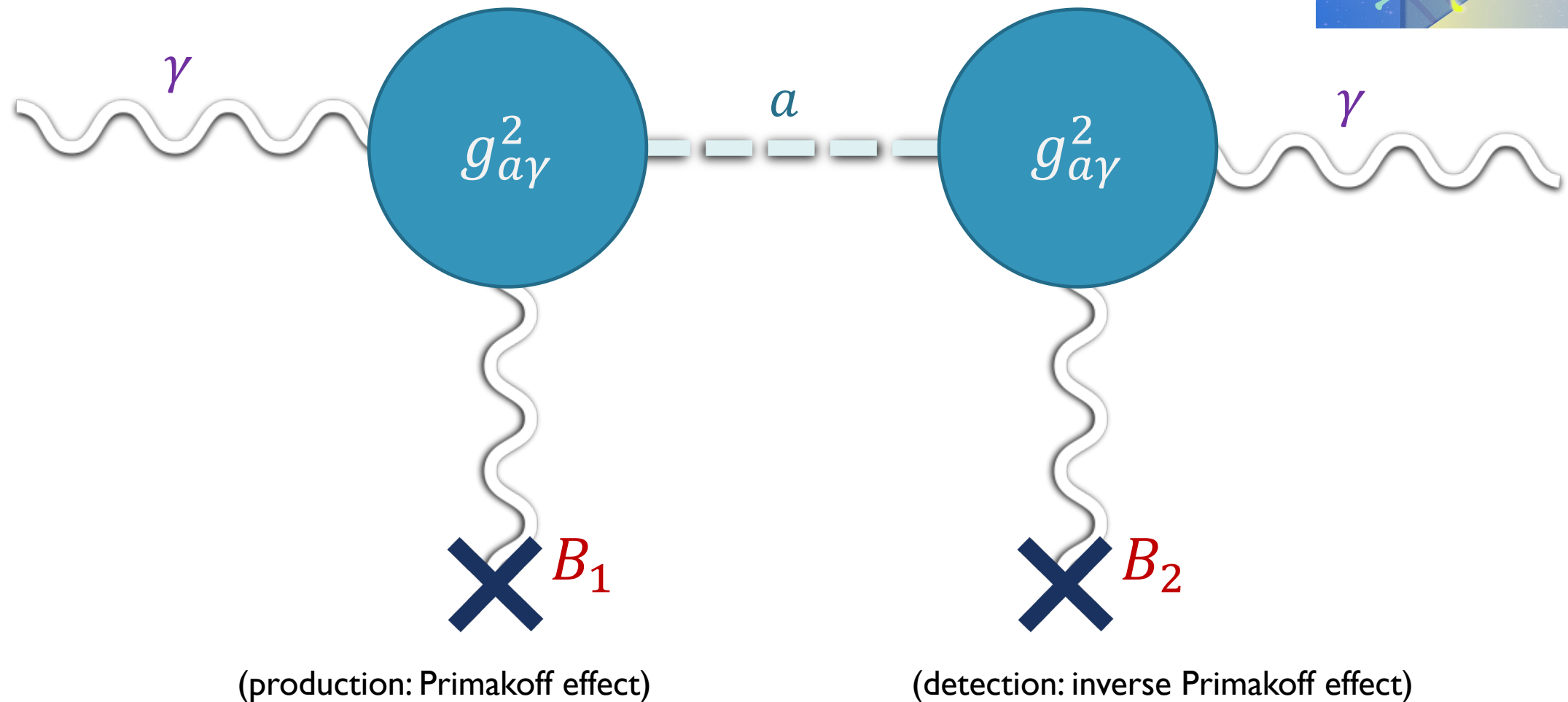
- ❖ In the presence of an external magnetic field, B , ALPs undergo a conversion into gamma-rays:

$$\mathcal{L}_{a\gamma} \supset -\frac{1}{4} g_{a\gamma} \mathbf{E} \cdot \mathbf{B} a$$

where $g_{a\gamma}$ is ALP-photon coupling rate, and a is the axion field strength.



OBSERVING ALPs WITH GAMMA-RAYS



TAKE-AWAY POINTS ABOUT ALPs

- Viable *cold* dark-matter candidate, belonging to the family of WISPs (weakly-interacting sub- eV particles)
- ALPs convert into photons in the presence of a magnetic field (inverse Primakoff process)
- Gamma-ray observations can probe ALP parameter space

TALK OUTLINE

- Axion-like particles: Introduction and motivation
 - 1. *Fermi-LAT* Low Energy Technique: Sensitivity study
 - 2. Sensitivity of the future MeV instruments
 - 3. Gamma-ray Bursts as ALP factories: what has *Fermi* seen so far?
 - 4. *Fermi-LAT* GRB pre-cursor analysis
- Conclusions & future work

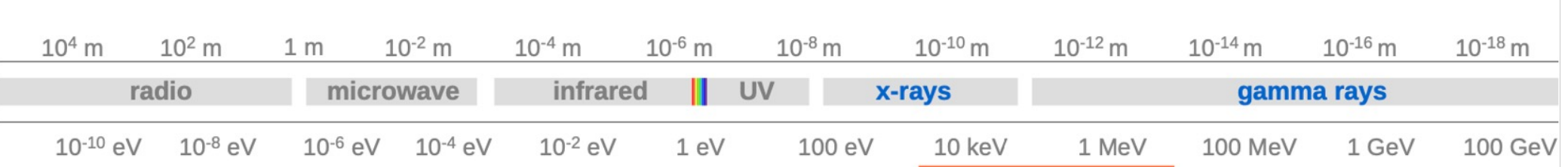
TALK OUTLINE

- Axion-like particles: Introduction and motivation
 - *Fermi-LAT* Low Energy Technique: Sensitivity study
 - Sensitivity of the future MeV instruments
 - Gamma-ray Bursts as ALP factories: what has *Fermi* seen so far?
 -  *Fermi-LAT* GRB pre-cursor analysis
- Conclusions & future work

HOW FAR CAN FERMI SEE?

Axion-like Particles from Core-collapse Supernovae:
Investigating *Fermi* Sensitivity with the LAT
Low-energy Technique

Crnogorčević et al. 2021 (PRD, [arXiv:2109.05790](#))



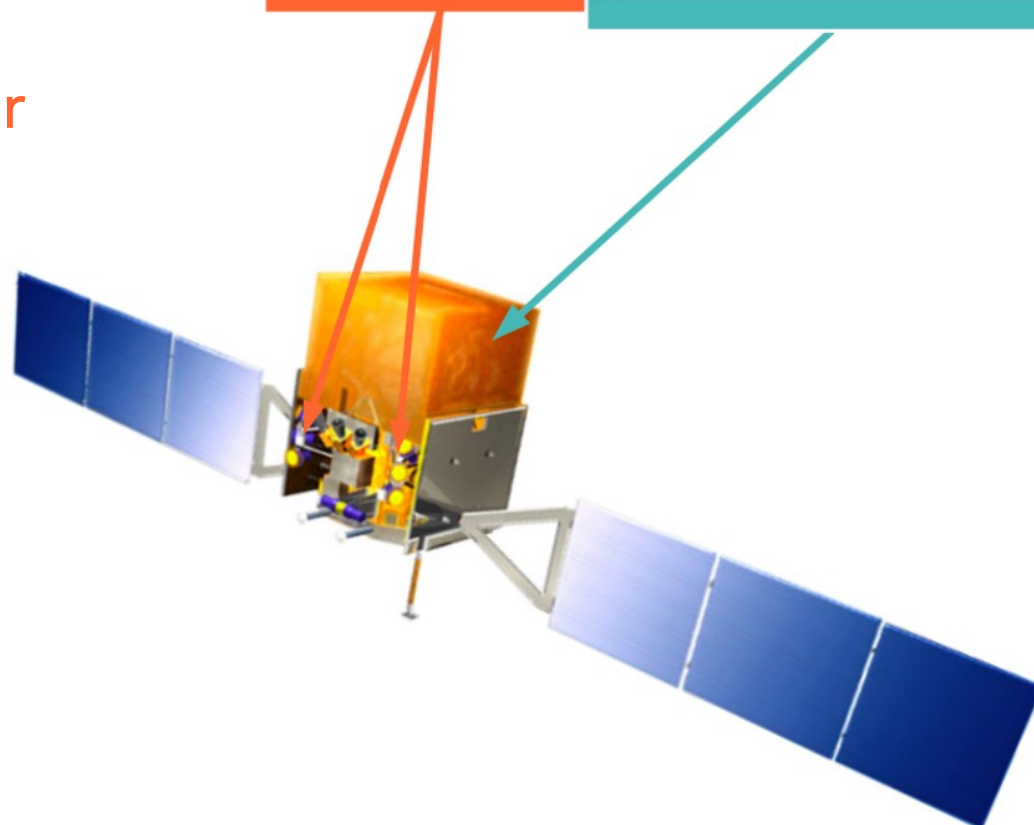
GBM Gamma-ray Burst Monitor

12 (NaI) + 2 (BGO) detectors

FoV: entire unocculted sky

8 keV to 40 MeV

~1500 bursts (~1 every day or two)



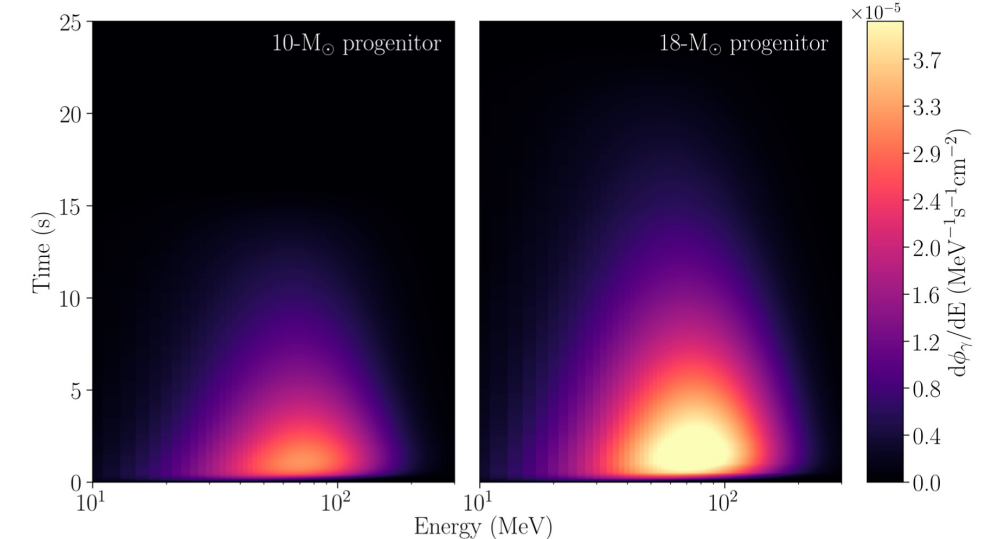
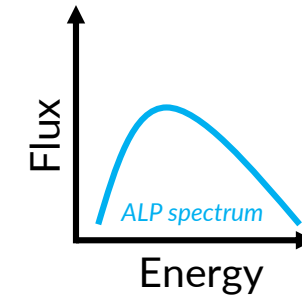
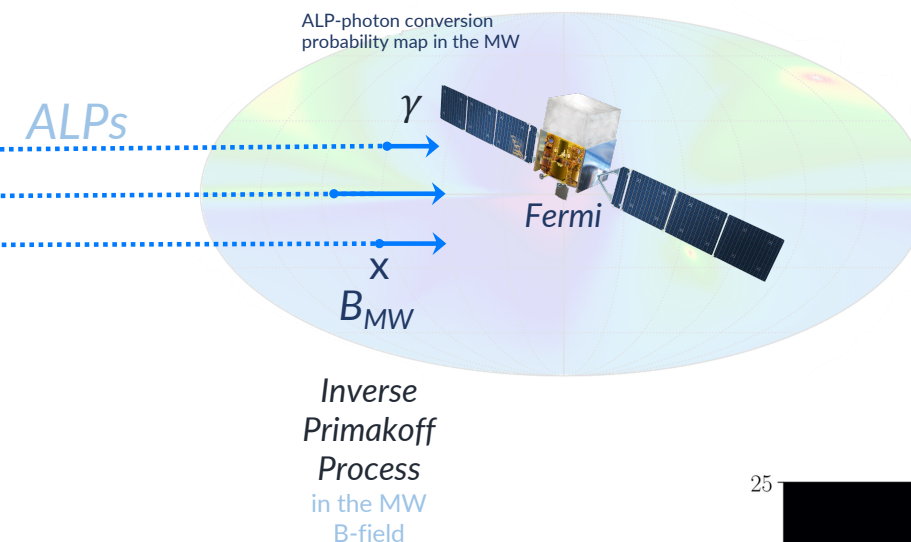
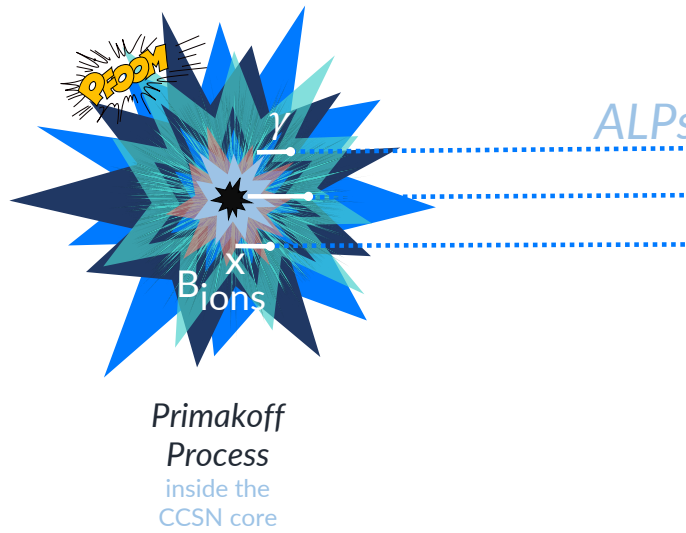
LAT Large Area Telescope

Pair-production telescope

FoV: 2.4 sr (~20% of sky)

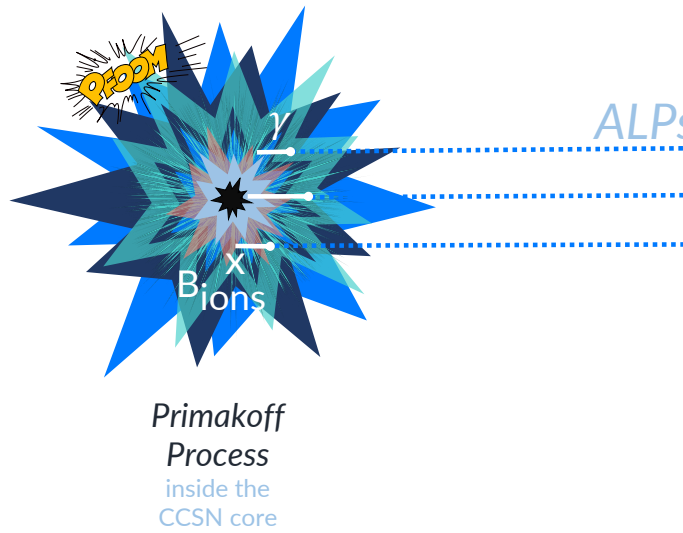
20 MeV to >300 GeV

MOTIVATION AND ASSUMPTIONS

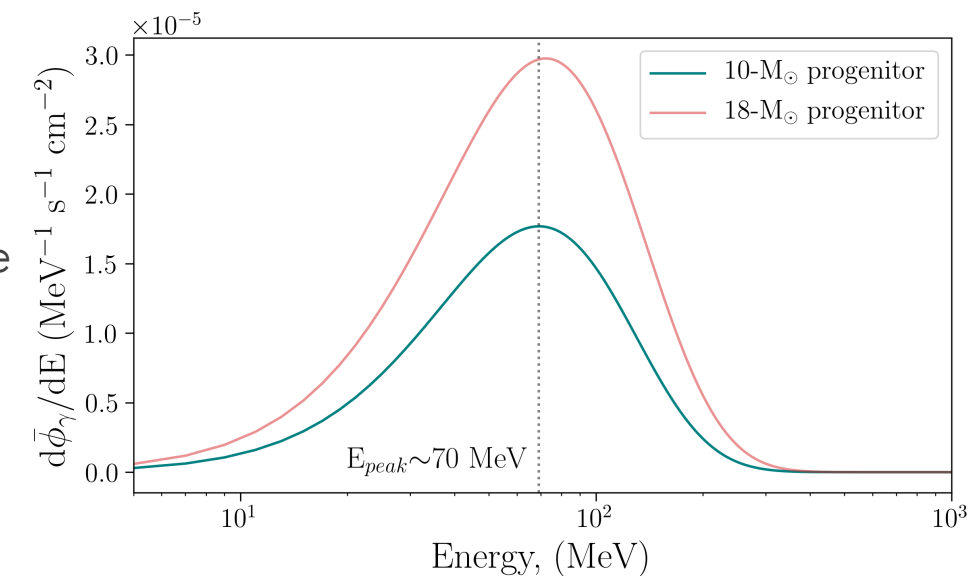
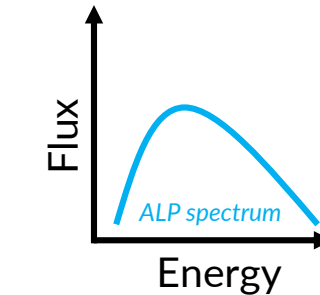


Observed evolution of the ALP-induced gamma-ray emission in time and energy in a core-collapse of a 10 and 18-M_\odot progenitor.

MOTIVATION AND ASSUMPTIONS

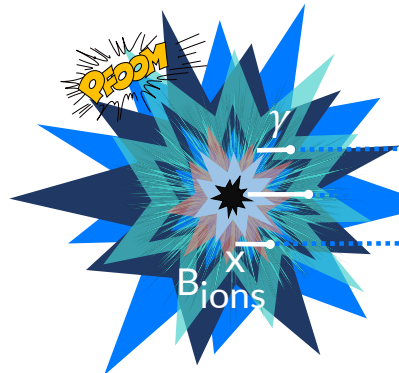


- **Motivation:** ALPs are theorized to have a unique spectral signature in the gamma-ray spectrum of a CCSN. No other known physical processes are predicted to produce such signature.

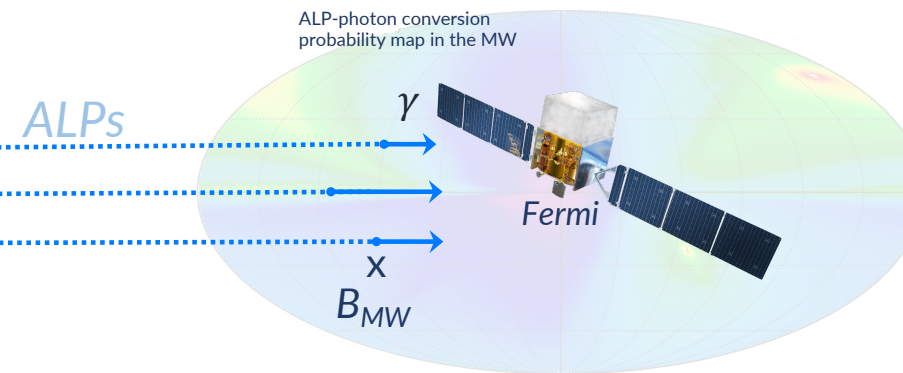


The observed ALP-induced gamma-ray spectrum for 10 and 18- M_\odot progenitors averaged over 10 seconds.

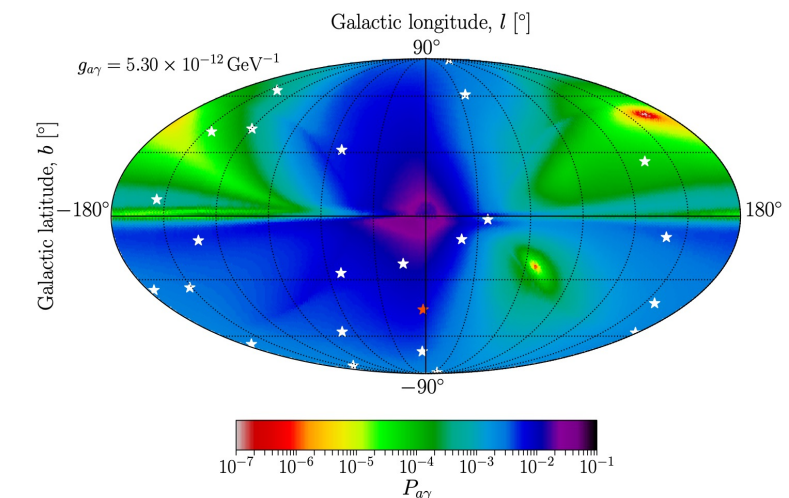
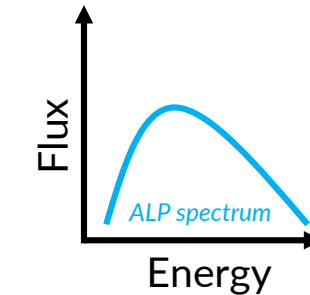
MOTIVATION AND ASSUMPTIONS



Primakoff
Process
inside the
CCSN core



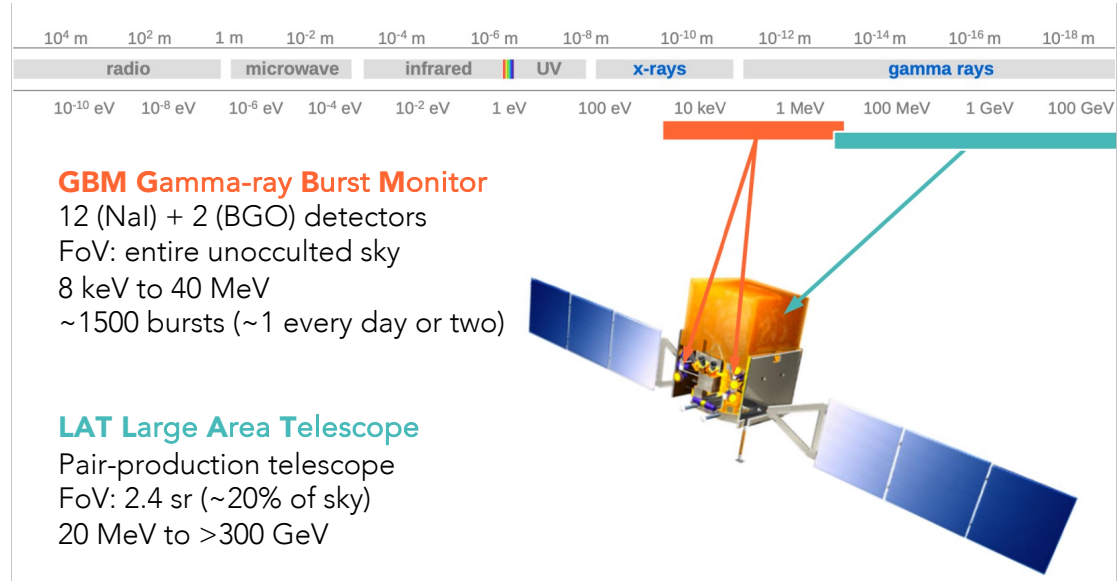
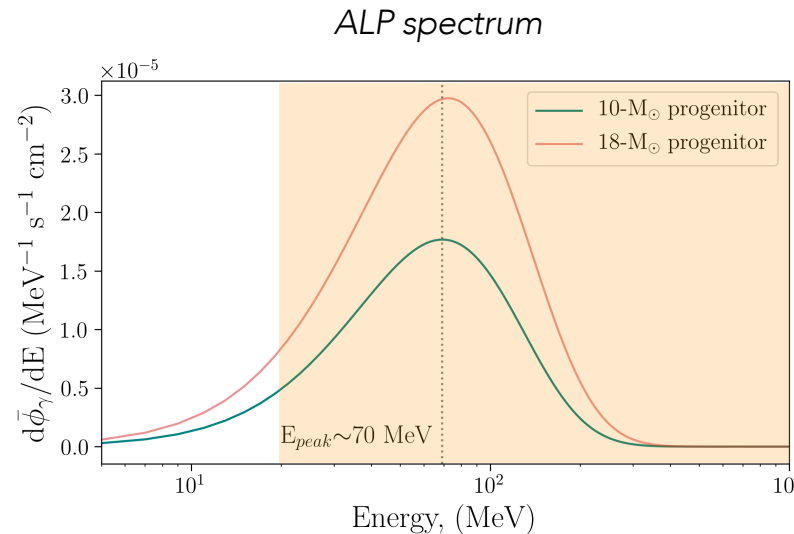
Inverse
Primakoff
Process
in the MW
B-field



‣ **Motivation:** ALPs are theorized to have a unique spectral signature in the gamma-ray spectrum of a CCSN. No other known physical processes are predicted to produce such signature.

‣ **Assumptions:**

magnetic fields: only considering the MW magnetic field, neglecting IGMF



LAT LOW ENERGY (LLE) TECHNIQUE

- Standard LAT analysis: >100 MeV (Meyer et al. 2020). **LLE analysis: >20 MeV**
- Goal: maximizing the effective area of the LAT instrument in the low-energy regime
 - Relaxing requirements on the background rejection: more signal, but also more background!
 - Only works for pulse-like sources (i.e., transients)
 - Direction information necessary
 - Additional response functions needed (Monte Carlo simulations of a bright point source at the position of interest)
- Systematics: flux values on average lower than those from the standard LAT analysis

SENSITIVITY TESTING: ANALYSIS & RESULTS

Model backgrounds from the considered LLE-detected GRB sample.

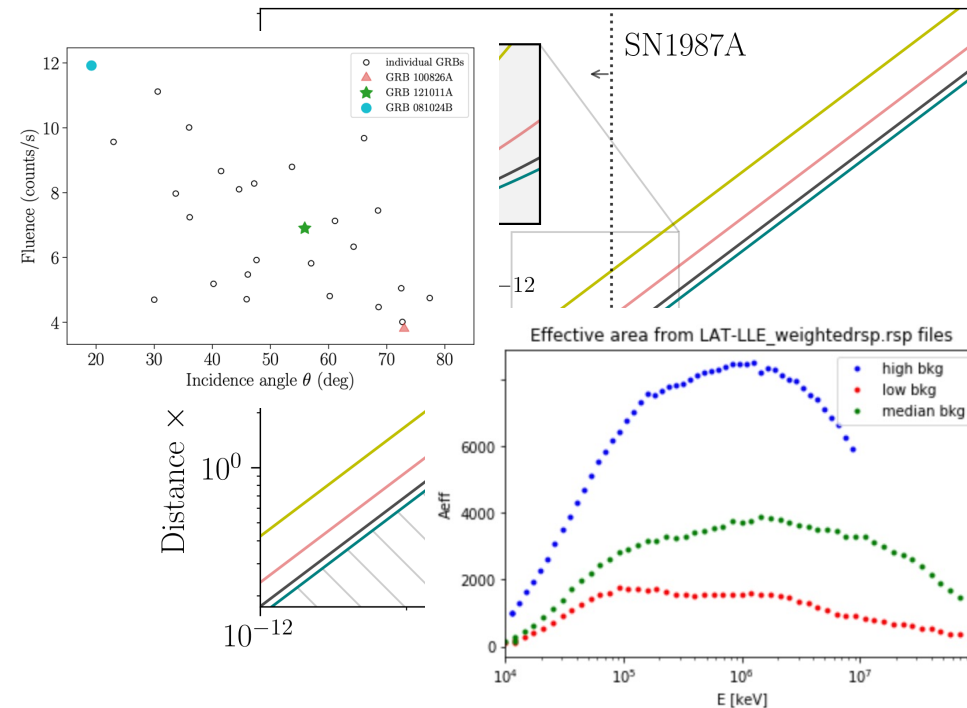
Find the min, max, and median background levels.

Produce ALP signal normalized by a value from the normalization grid for 10-and 18-solar-mass progenitors.

Produce 2000 realizations of the background+ALP spectrum and their corresponding (GRB) response functions (XSPEC fakeit function.)

Fit the ALP and the “background-only” model. Apply Wilks’ Theorem and LLR test to find for which normalization ALP model is preferred.

Find the coupling-distance parameter space for that normalization.



Background level	Conversion probability, $P_\gamma(g_0)$	Distance limit (Mpc) 10 M _⊙	Distance limit (Mpc) 18 M _⊙
Low	0.1	4.4	6.5
Median	0.1	4.9	7.1
High	0.1	6.6	9.7
Low	0.05	3.1	4.6
Median	0.05	3.5	5.0
High	0.05	4.7	6.9
Low	0.01	1.4	2.1
Median	0.01	1.5	2.3
High	0.01	2.1	3.1
Low	0.001	0.4	0.7
Median	0.001	0.5	0.7
High	0.001	0.7	1.0

$$N_{\text{ALP}} \propto \frac{g_{a\gamma}^4}{d^2}$$

Crnogorčević et al. 2021 (PRD, [arXiv:2109.05790](https://arxiv.org/abs/2109.05790))

RESULTS I. *HOW FAR CAN FERMI SEE?*

- **Tools:** a developed pipeline for calculating distance limits for the current and future gamma-ray instruments for the given ALP mass and coupling
- **Novel results:** using a transient data class as observed by *Fermi* to probe its sensitivity. Results are consistent with the analysis using the standard LAT data [Meyer et al. 2016].
- **Good scientific case for the future instruments:** they need more sensitivity in the MeV region in order to be able to increase the statistics of sources considered

TALK OUTLINE

- Axion-like particles: Introduction and motivation
 - 1. *Fermi-LAT* Low Energy Technique: Sensitivity study
 - 2. Sensitivity of the future MeV instruments**
 - 3. Gamma-ray Bursts as ALP factories: what has *Fermi* seen so far?
 - 4. *Fermi-LAT* GRB pre-cursor analysis
- Conclusions & future work

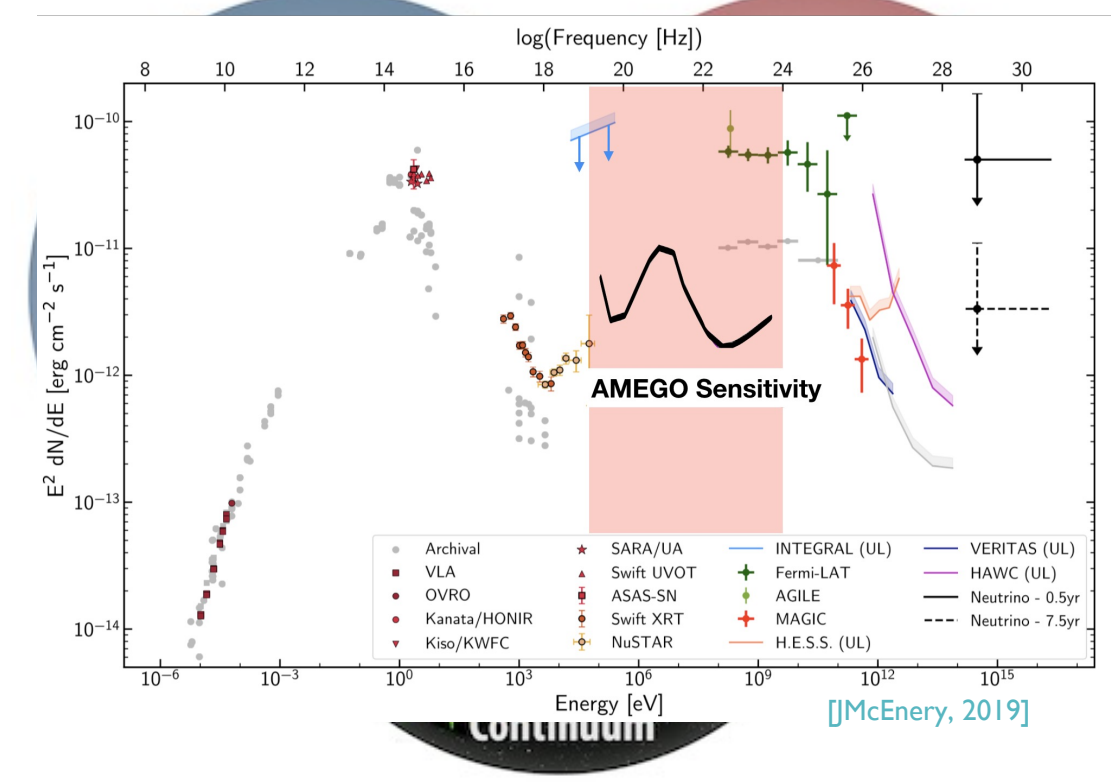
ADDITIONAL CONSIDERATION



Additional considerations: All-sky Medium Energy Gamma-ray Observatory (AMEGO) sensitivity analysis; motivation outlined the [Snowmass 2021 Letter of Interest](#) (Prescod-Weinstein et al. 2021, incl. Crnogorčević)

Quick factsheet about AMEGO:

- Probe-class mission concept
- High-sensitivity (200 keV – 10 GeV)
- Wide FoV, good spectral resolution, polarization
- Multimessenger astronomy (NS mergers, SNe, AGN)
- Order-of-magnitude improvement compared to previous MeV missions



ADDITIONAL CONSIDERATIONS

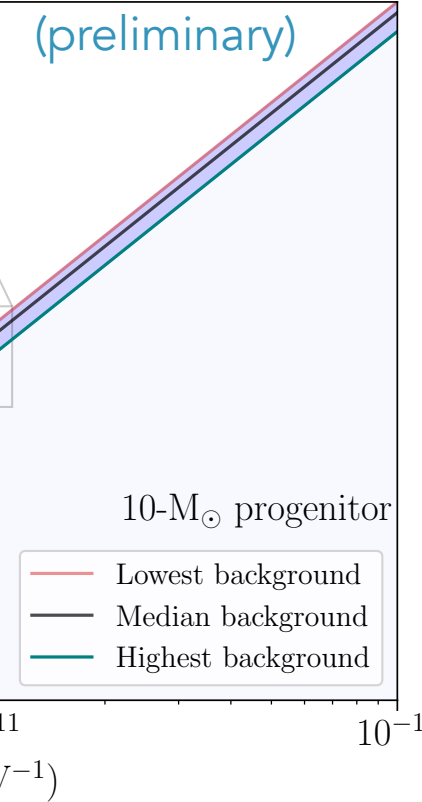
Additional considerations: All-sky Medium Energy Gamma-ray Observatory (MEGO-X) outlined the [Snowmass 2021 Letter](#)

- For a 10-solar mass progenitor, sensitivity levels comparable to LAT in the low energy range

Distance limit improved by a factor of

MEGO-X
ALL-SKY MEDIUM ENERGY GAMMA-RAY OBSERVATORY

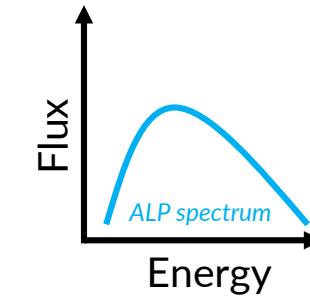
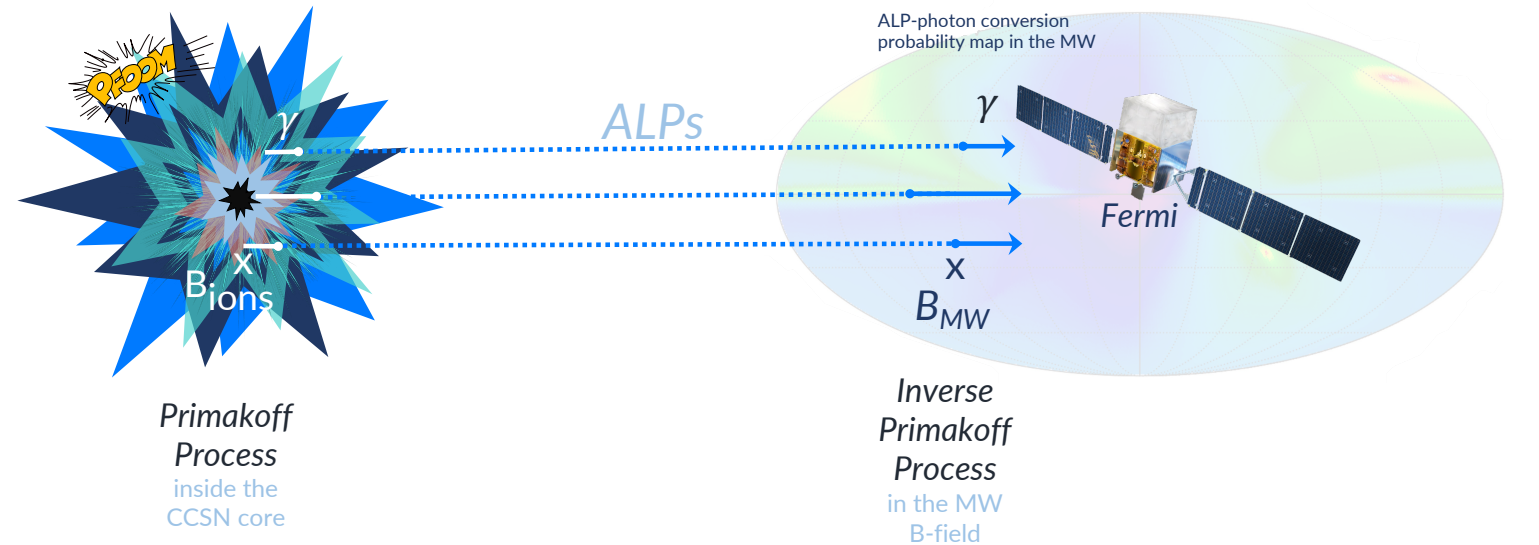
(sensitivity analysis; motivation
(Crnogorčević)



TALK OUTLINE

- Axion-like particles: Introduction and motivation
 - 1. *Fermi-LAT* Low Energy Technique: Sensitivity study
 - 2. Sensitivity of the future MeV instruments
 - 3. Gamma-ray Bursts as ALP factories: what has *Fermi* seen so far?**
 - 4. *Fermi-LAT* GRB pre-cursor analysis
- Conclusions & future work

MOTIVATION AND ASSUMPTIONS



CCSNe \rightarrow long Gamma-ray Bursts (GRBs)

GRB ANALYSIS

Property	Selection Criterion
Distance	unassociated (no redshift)
Detection significance	$\geq 5\sigma$ in LAT-LLE ($\gtrsim 30$ MeV)
Observed time interval	\geq duration of the burst
Burst duration	long GRBs ($T_{95} \gtrsim 2$ seconds)

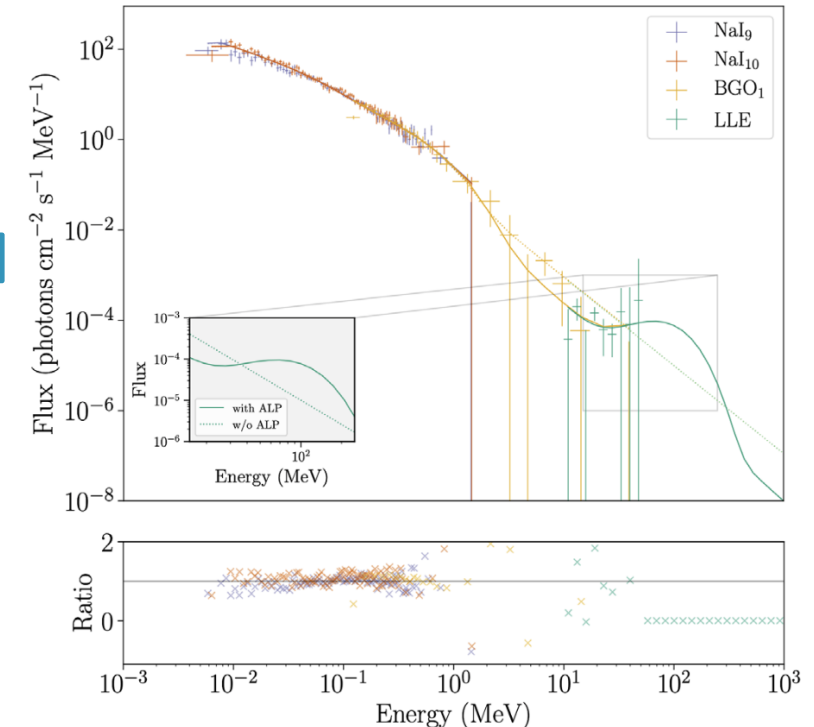
Initial sample: 186 LAT-detected GRBs

Applying the selection criteria

24 GRBs

GRB ANALYSIS RESULTS

GRB	T ₉₅ (s)	Best model(no ALP)	grbm parameters			
			α_1	α_2	E _c (keV)	LLR
080825C	22.2	grbm	-0.65 ^{+0.05} _{-0.05}	-2.41 ^{+0.04} _{-0.04}	143 ⁺¹³ ₋₁₂	0.2
090217	34.1	grbm	-1.11 ^{+0.04} _{-0.04}	-2.43 ^{+0.03} _{-0.04}	16 ⁺¹³ ₋₈	0.1
100225A	12.7	grbm	-0.50 ^{+0.25} _{-0.21}	-2.28 ^{+0.07} _{-0.09}	223 ⁺¹¹² ₋₆₈	0.0
100826A	93.7	grbm+bb	-1.02 ^{+0.04} _{-0.04}	-2.30 ^{+0.03} _{-0.04}	484 ⁺⁷² ₋₆₃	0.0
101123A	145.4	grbm+cutoffpl	-1.00 ^{+0.07} _{-0.08}	-1.94 ^{+0.15} _{-0.12}	187 ⁺⁷⁴ ₋₆₂	5.8
110721A	21.8	grbm+bb	-1.24 ^{+0.02} _{-0.01}	-2.29 ^{+0.03} _{-0.03}	1000 ⁺²⁸ ₋₃₉	0.0
120328B	33.5	grbm+cutoffpl	-0.67 ^{+0.06} _{-0.05}	-2.26 ^{+0.05} _{-0.05}	101 ⁺¹² ₋₁₃	0.0
120911B	69.0	grbm	-2.50 ^{+0.92} _{-1.04}	-1.05 ^{+0.63} _{-0.38}	11 ⁺¹⁰ ₋₂	0.0
121011A	66.8	grbm	-1.08 ^{+0.10} _{-0.21}	-2.18 ^{+0.11} _{-0.16}	997 ⁺⁸⁴ ₋₂₆	0.0
121225B	68.0	grbm	-2.38 ^{+1.02} _{-0.40}	-2.45 ^{+0.06} _{-0.07}	11 ⁺⁸⁹ ₋₃	0.0
130305A	26.9	grbm	-0.76 ^{+0.03} _{-0.03}	-2.63 ^{+0.06} _{-0.06}	665 ⁺⁶¹ ₋₅₅	0.0
131014A	4.2	grbm	-0.55 ^{+0.33} _{-0.98}	-2.65 ^{+0.17} _{-0.19}	255 ⁺³⁶ ₋₁₁	0.63
131216A	19.3	grbm+cutoffpl	-0.46 ^{+0.28} _{-0.24}	-2.67 ^{+1.94} _{-0.94}	178 ⁺⁷⁷ ₋₉₂	0.0
140102A	4.1	grbm+bb	-1.10 ^{+0.12} _{-0.09}	-2.41 ^{+0.16} _{-0.11}	206 ⁺⁶⁵ ₋₉₂	2.3
140110A	9.2	grbm	-2.49 ^{+1.64} _{-1.59}	-2.19 ^{+0.20} _{-0.22}	11 ⁺²³ ₋₃	0.0
141207A	22.3	grbm+bb	-1.21 ^{+0.09} _{-0.06}	-2.33 ^{+0.11} _{-0.13}	999 ⁺¹⁸ ₋₇₀	0.0
141222A	2.8	grbm+pow	-1.57 ^{+0.03} _{-0.02}	-2.83 ^{+0.46} _{-1.74}	9971 ⁺³⁹⁰ ₋₈₃₂	0.0
150210A	31.3	grbm+pow	-0.52 ^{+0.04} _{-0.05}	-2.91 ^{+0.11} _{-0.38}	1000 ⁺⁵¹⁷ ₋₂₃₄	0.0
150416A	33.8	grbm	-1.18 ^{+0.04} _{-0.04}	-2.36 ^{+0.13} _{-0.21}	999 ⁺¹⁸⁷ ₋₂₆₉	0.0
150820A	5.1	grbm	-0.99 ^{+0.56} _{-1.30}	-2.01 ^{+0.82} _{-0.27}	303 ⁺⁶¹ ₋₃₉	0.0
151006A	95.0	grbm	-1.35 ^{+0.06} _{-0.03}	-2.24 ^{+0.07} _{-0.08}	998 ⁺³³ ₋₈₄	0.0
160709A	5.4	grbm+cutoffpl	-1.44 ^{+0.18} _{-0.12}	-2.18 ^{+0.15} _{-0.18}	9940 ⁺³⁷³ ₋₅₁₁	1.0
160917A	19.2	grbm+bb	-0.78 ^{+3.45} _{-1.40}	-2.39 ^{+0.20} _{-0.10}	994 ⁺⁶³⁴ ₋₂₁₆	0.9
170115B	44.8	grbm	-0.80 ^{+0.02} _{-0.04}	-3.00 ^{+0.10} _{-0.07}	1000 ⁺²²⁶ ₋₁₀₆	2.8



global p-value of ~ 0.3 , indicating that this observation is not statistically significant.

TALK OUTLINE

- Axion-like particles: Introduction and motivation
 - 1. *Fermi-LAT* Low Energy Technique: Sensitivity study
 - 2. Sensitivity of the future MeV instruments
 - 3. Gamma-ray Bursts as ALP factories: what has *Fermi* seen so far?
 - 4. *Fermi-LAT* GRB pre-cursor analysis**
- Conclusions & future work

WHEN TO SEARCH FOR ALPs?

- The ALP signal should be coincident with the neutrino emission from a supernova
 - For extragalactic SN, no neutrino signal is expected current generation of neutrino detectors [Kistler et al. 2011]; in the Milky Way ~2-3 SNe/century [Türler et al. 2006]
- We can use optical light curves of extragalactic SNe to determine explosion times
 - Method introduced in [Cowen et al. 2010] and applied in the context of ALP searches in [Meyer et al. 2020], resulting in most stringent upper limits on the light ALP parameter space
- We can look for an ALP signal at the time of GRB emission, assuming that the GRB is ALP-induced
 - Method introduced in [Crnogorčević et al. 2021] using a sample of LAT-detected GRBs. No significant (5σ) detections reported

→ A study of GBM/LAT bursts with precursor emission: a systematic search for ALP excess in targeted time windows before presumed gamma-ray jet emission

LIGHT AT THE END OF THE TUNNEL

Search for Axion-like Particle Dark Matter in Precursor
Emission of Long Gamma-ray Bursts

Crnogorčević et al. (*in prep.*)

Fermi GI Cycle 15 (Pl: Crnogorčević)

GOALS

Precursor emission in Fermi-detected GRBs: a comprehensive search for ALP signatures in different time windows

- Multiple theoretical models have been proposed to address the question of precursor emission in GRBs, none conclusive [e.g., Koshut et al. 1995, Lazzati et al. 2005, Burlon et al. 2008, Troja et al. 2010, Tsang et al. 2011, Coppin et al. 2020]
- We propose that the precursor emission **may be accounted for by ALPs**
- Assumption: that the ALP breakout time corresponds to the pre-cursor time tag
- **Goals:**
 1. Determine whether an addition of an ALP model component improves the fit for the GRB precursor emission in the LLE data
 2. Compute constraints on the ALP parameter space from a consideration of LAT/LLE emission at the time of the expected precursor

WHAT HAVE WE DONE SO FAR?

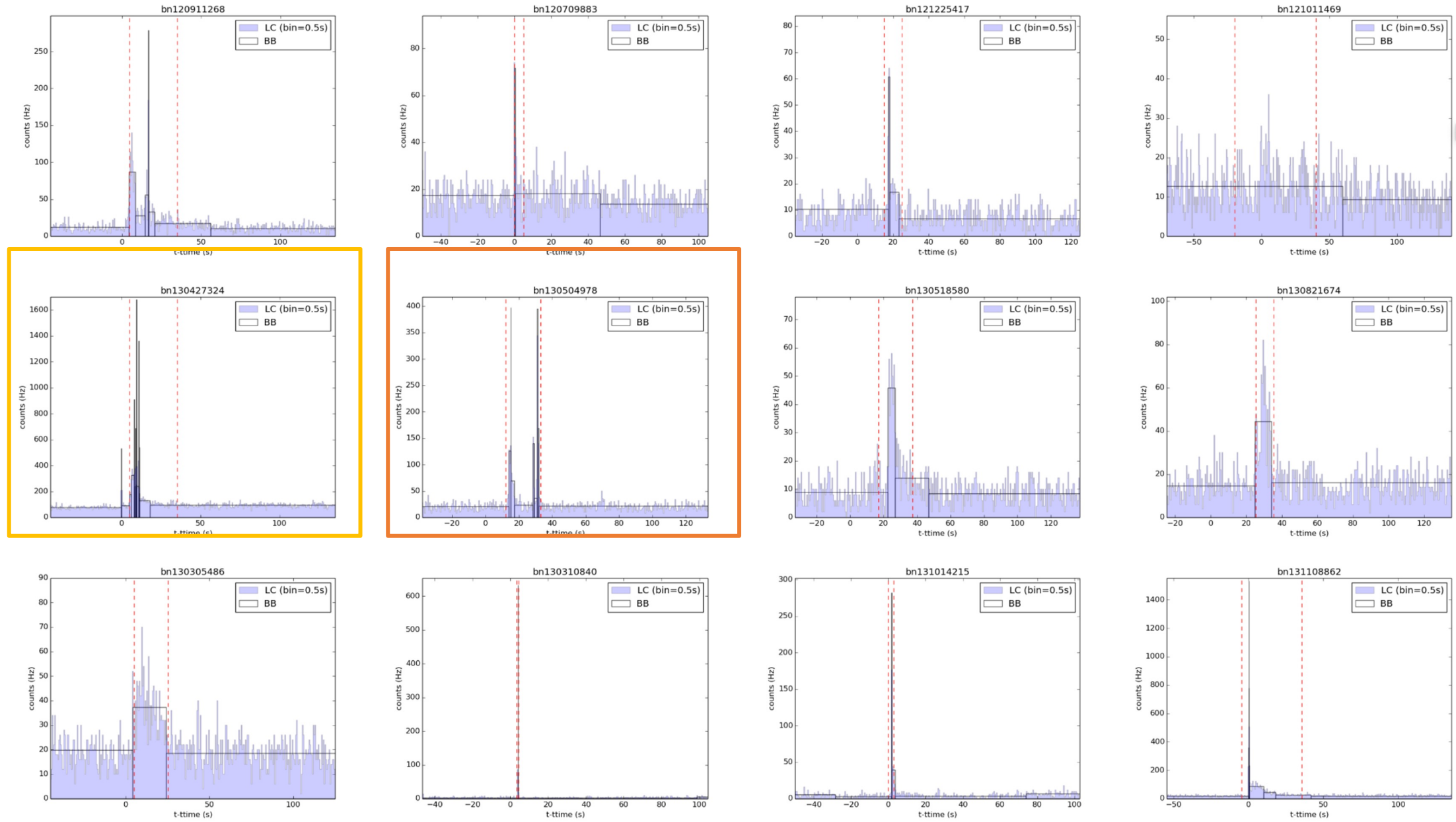
Bayesian Block Analysis on the LLE-detected GRBs

- Using the code developed by Vianello 2014
- Allows for a selection of time bins for a time-resolved spectra
 - Default output: T90 interval (i.e. time in which 90% of the GRB fluence is emitted)
 - Time range: $[T_{\text{FoV}} \text{ to } T_0 - 10 \text{ sec}]$ [Zhang et al. 2019]
 - T_{FoV} : time the source enters LAT's FoV
 - T_0 : trigger time
- Considered so far: LLE-detected GRBs (56)

→ Goal: search for excess signal!

Example trial runs

(Note that all the following plots are in the $[T_0 \pm 400 \text{ s}]$)

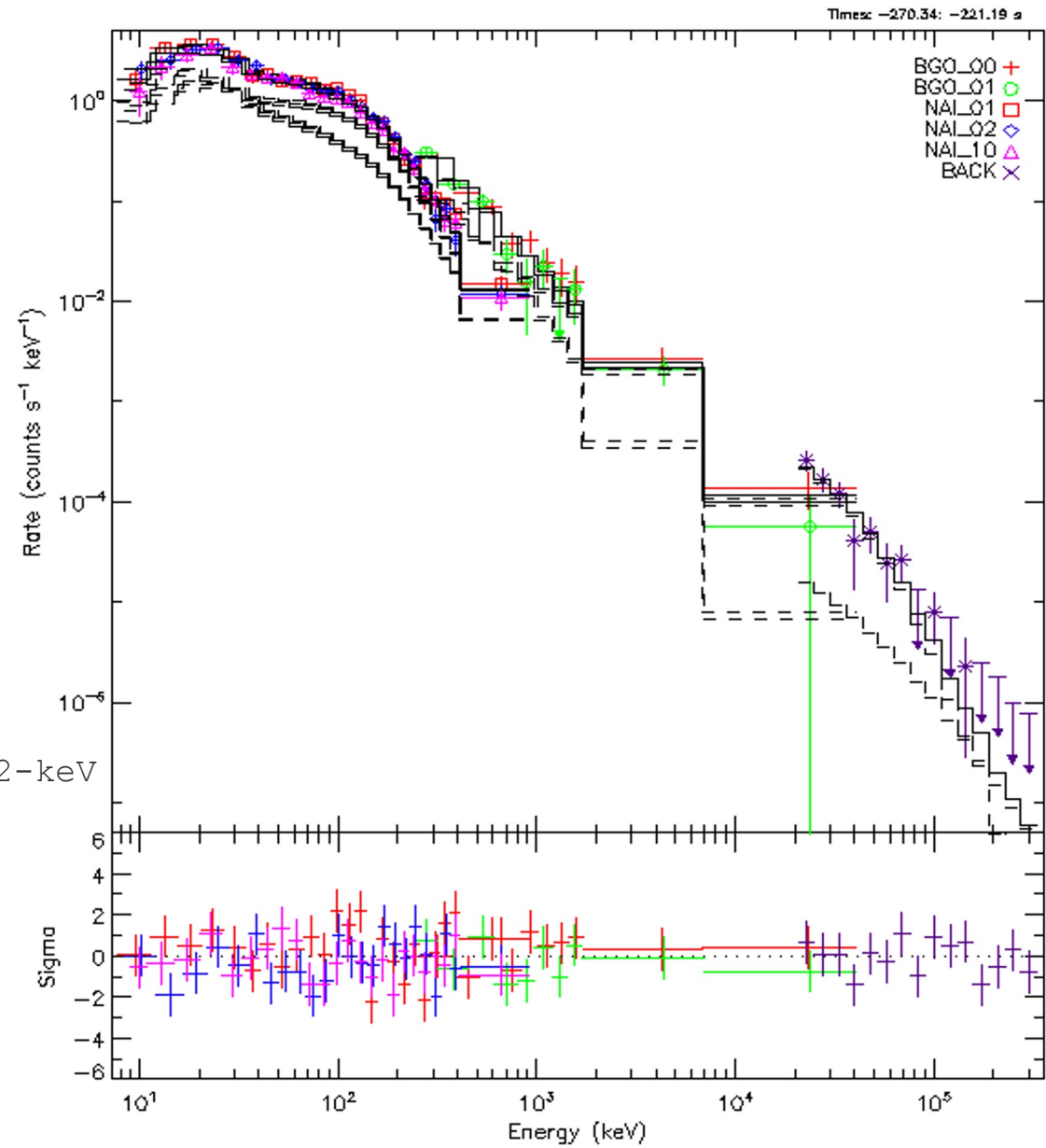


GRB 120624

- precursor emission in GBM & LLE
- precursor fit ($T_0 - 270$ to $T_0 - 220$ seconds)
- **Best fit: Band function**

TERM: Band's GRB, Epeak

Amplitude	VARY	0.007494 +/-	0.000535 p/s-cm ² -keV
Epeak	VARY	387.9 +/-	51.2 keV
alpha	VARY	-0.5282 +/-	0.216
beta	VARY	-2.597 +/-	0.320



Searching for excess signal in precursor emission?

Spectral analysis complete for GRBs up to 2018 (a total of 56 GRBs)

Summary:

- No “significant” detections
 - out of 56 GRBs with a precursor, 41 have precursors in GBM (we should not expect ALP emission)
- What is a significant detection for a subthreshold emission?
 - This question requires a bit of thought: the only statement we can make here is that the ALP spectral model fits the precursor emission better than the traditional GRB models; however, this does not imply a detection. Additional crosschecks would be required (some mentioned in the previous meeting: e.g. stacking)

Upper-limit analysis

Goal 2: consider LAT/GBM/Swift GRBs and use the standard LAT data analysis

Selection criteria:

1. Long GRBs ($T90 > 2$ seconds)
2. Redshift < 0.6 (for a competitive coupling, $g < 2 \times 10^{-10}$ GeV $^{-1}$)
3. In LAT's FoV at least 10 seconds prior to the trigger time

→ 9 LAT bursts, 12 GBM bursts

- We consider light ALPs, hypothetically produced in CCSNe, and converted into gamma-rays in the MW magnetic field
- We test LAT sensitivity, including the LLE data cut and extending into energies relevant to the ALP spectral signature (a few tens of MeV)
- **Result: LLE can reach up to ~10 Mpc for detecting ALPs**
 - driven by the dominating background in the LLE data & decreased effective area at high incidence angles
 - Good science case for future MeV instruments (AMEGO-X, etc.)
 - We conduct ALP fitting to the unassociated, long, LLE-detected GRBs
- **Result: No statistically significant detection in our sample**
 - highly unlikely that the GRB trigger time is the same as the ALP emission time (most of the selected GRBs are well-fit by the common GRB models)
 - Pre-cursor emission in LLE. **Preliminary results: no detection!**
 - Current work: upper-limit analysis at the time of precursor with LAT standard data!

THANK YOU!

CROSS-CORRELATING ASTROPHYSICAL NEUTRINOS & FERMI UNRESOLVED GAMMA-RAY SKY

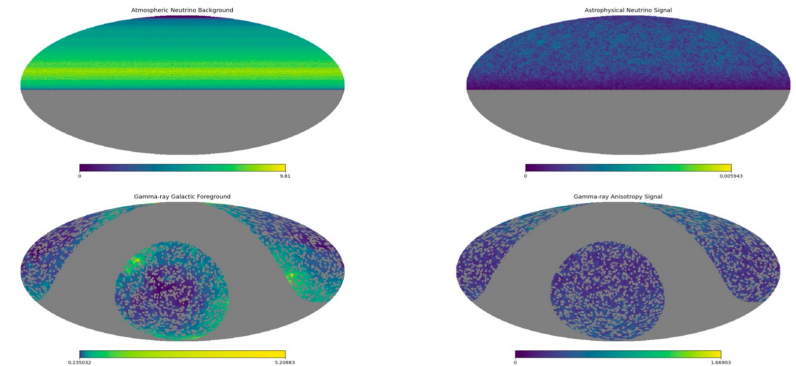
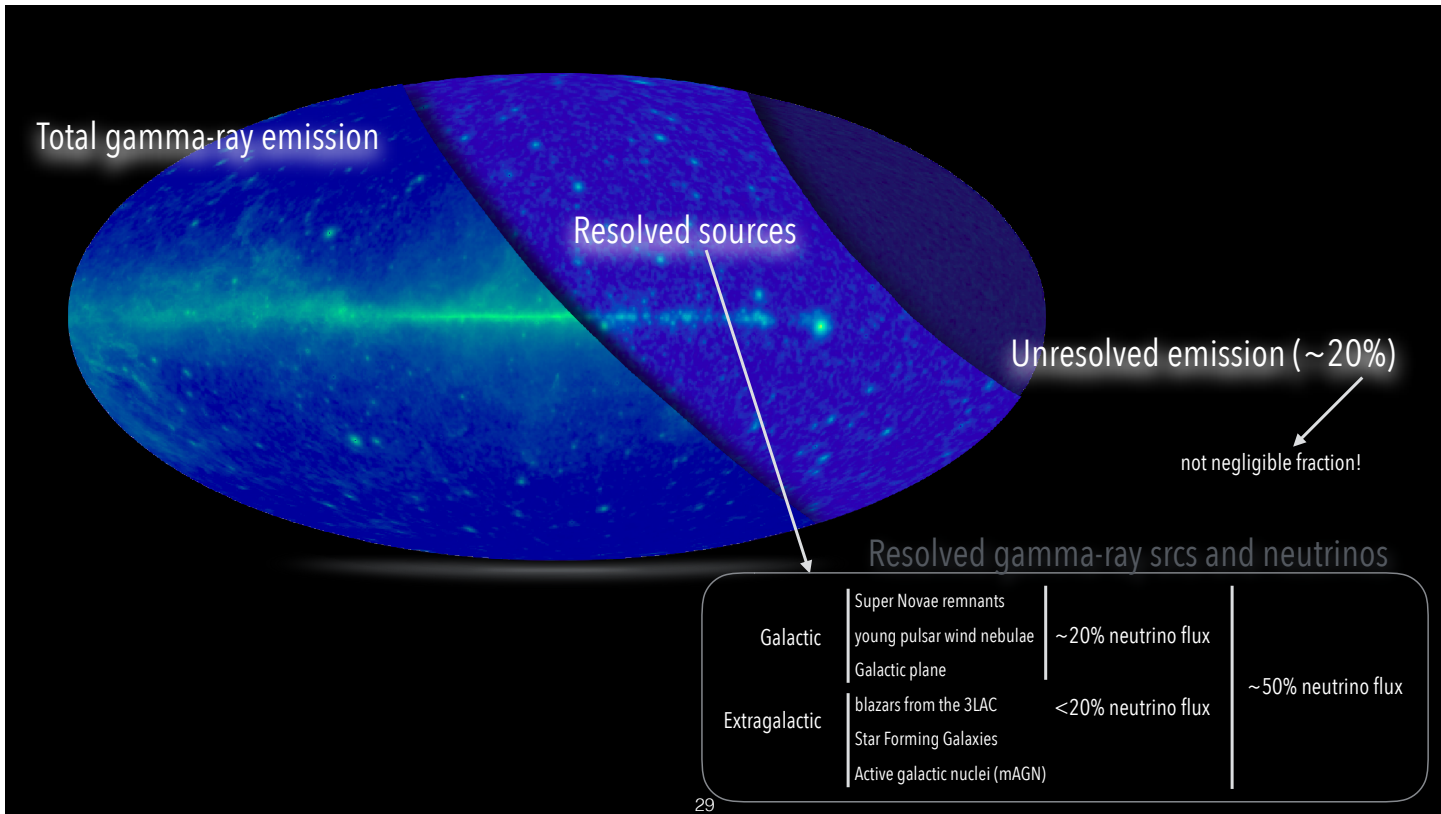


Fig. 7.— All-sky expected counts maps, in counts per $0.458^{\circ}2$ pixel (HEALPix $nside=128$) for simulated atmospheric neutrino (top left), astrophysical neutrino (top right), galactic gamma-ray foreground (bottom left) and gamma-ray signal (bottom right). The grey regions mark the masked pixels. See e.g. (Fang et al. 2020) for details on mask choice.

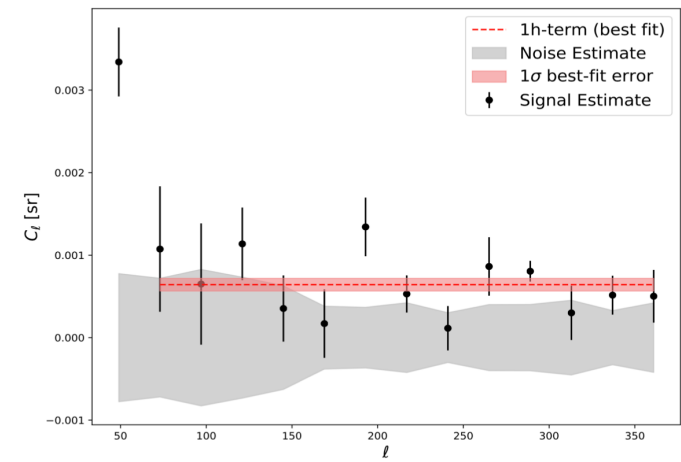


Fig. 8.— Comparison of expected signal and noise levels for cross-correlation of simulated 10-year neutrino data with gamma-ray data. The red dashed line and the red shaded band are the best fit and the relative 1σ error for a 1halo-term component, as described in the *halo model* formalism (Cooray & Sheth 2002).

CATCHING THE NEXT WAVE

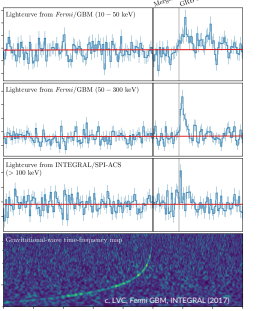
GWTC-3 follow-ups with GBM & BAT

MOTIVATION

- Since the coincident detection of gravitational waves (GWs) from a binary neutron-star (BNS) merger, (GW170817), and the corresponding short gamma-ray burst (GRB170817A), **detecting an analogous event has been a trending research topic in the multimessenger community**
- The standard trigger pipelines on the *Fermi*'s Gamma-ray Burst Monitor (GBM) and *Swift*'s Burst Alert Telescope (BAT) report no statistically significant (i.e., 5- σ) detections for any of the GW triggers reported in the Third Gravitational Wave Transient Catalog (GWTC-3)

GOALS

1. Combine GBM trigger & sub-threshold and BAT rate analyses to search for excess emission coincident with GW triggers in GWTC-3
2. Put constraints on the progenitor's theoretical model



Gamma-ray searches with *Fermi* GBM

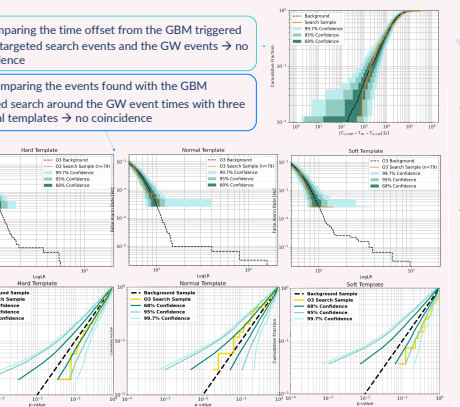
Why Fermi GBM?
+ ~full-sky field of view
+ energy coverage spanning the peak of GRB emission

y-ray searches
- Using Fermi GBM triggers and two threshold searches:
 - Targeted: scans -1 to 30 sec around a trigger time
 - Untargeted: a blind search of GBM data
→ Determined if there is any excess y-ray emission coincident with GWTC-3 events

ranking statistic (R)
→ R is mapped to a p-value and compared to the cumulative fraction
→ no coincident events.

$$R = \frac{P_{\text{astro}} \times p_{\text{vis}} \times p_{\text{assoc}}}{|\Delta t - D| \times \text{FAR}_{\text{GBM}}}$$

Equation: the probability the GW event is astrophysical (P_{astro}) visible to GBM (p_{vis}) that GW and GBM trigger at the same time (Δt), the GW-GBM time offset (D), GBM event duration (D), and the GBM False Alarm Rate (FAR_{GBM})



Hard X-ray searches with *Swift* BAT

Why Swift BAT?
+ excellent localization sensitivity (~arcminute for detected GRBs)
+ energy coverage overlaps with the low-energy end of *Fermi* GBM

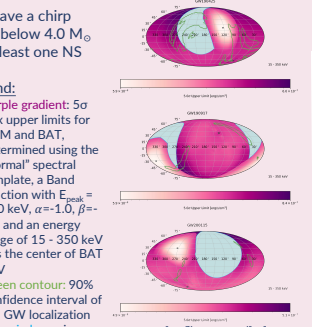
1. Extract BAT raw light curves in 64-ms time bins → rebin to match GBM time-steps (0.5 s)
 2. Calculate average counts and standard deviation using the data from -1 to +30 seconds around the trigger time
 3. Use NITRATES to produce response functions for rate data, as a function of the incidence angle onto the BAT detector plane
 4. Calculate the expected counts using the Band function as the expected GRB model
 5. Simulate GRB spectra and find the corresponding flux
- Example of the upper-limit map: GW200311

Calculation of BAT upper limits

Example of the upper-limit map: GW200311

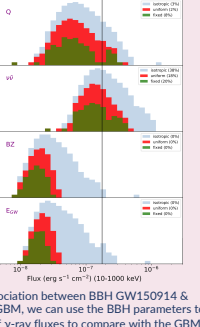
Joint upper-limit skymaps

E.g.: GW190425, GW190918, and GW200115



BBH modeling

EM radiation from binary-black-hole mergers?



Conclusions

- Using *Fermi* GBM triggers and sub-threshold searches, and *Swift* BAT's data to search for coincident y-ray emission with the GWTC-3 events, we **found no coincident detections**
- We calculated the **flux upper limits** for both GBM and BAT and present **joint upper-limit skymaps**
- Comparing the upper limits expectations from various BBH merger theoretical models we find that we can likely rule out the neutrino model for producing EM emission

References

- [1] Meegan et al. 2009;
- [2] Goldstein et al. 2019;
- [3] Barthelmy et al. 2005;
- [4] DeLaunay & Tohuvavohu 2021;
- [5] Connaughton 2016.



Thank you!

QUESTION III. *WHAT ELSE HAVE I BEEN UP TO?*

Multimessenger studies of the high-energy Universe

PROJECT I: SWIFT-BAT FOLLOW-UP OBSERVATIONS OF BINARY COALESCENCE EVENTS IN THE LIGO/VIRGO O3 RUN

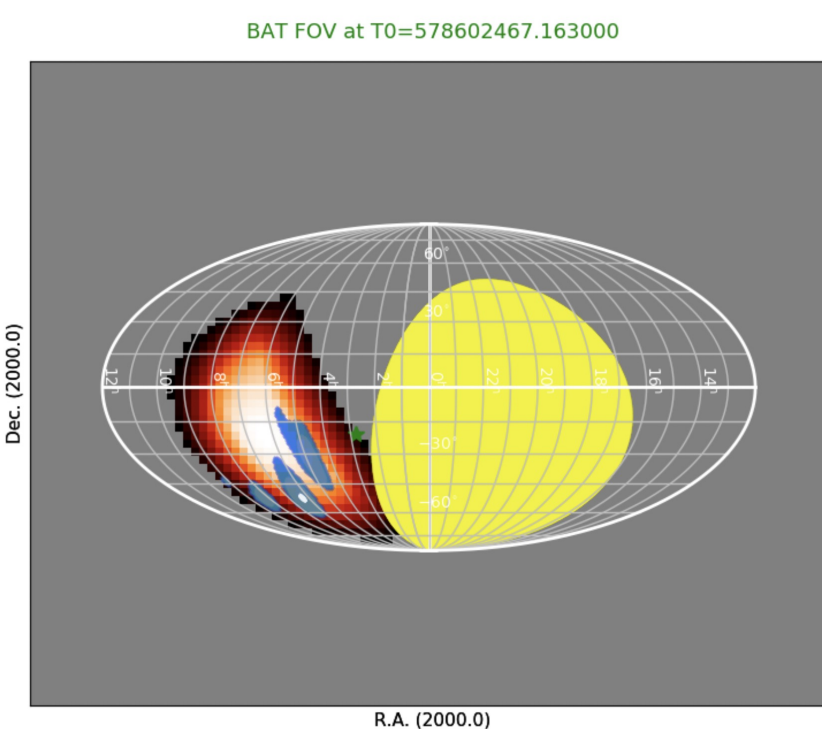
- Goal: Joint analysis between the Fermi GBM Team (led by C. Fletcher and J. Wood), and the Swift-BAT Team (led by **M. Crnogorčević** and R. Caputo) for follow-up observations to compact binary coalescence events identified by the Advanced LIGO and Advanced Virgo detectors during the third gravitational wave observing run.
- Results: to date, no new joint events beyond GRB/GW170817 have been found. Upper limits on flux for each of the gravitational wave triggers have been calculated. We intend place limits on potential EM emission from binary black hole mergers.

O3a Catalog gravitational-wave events

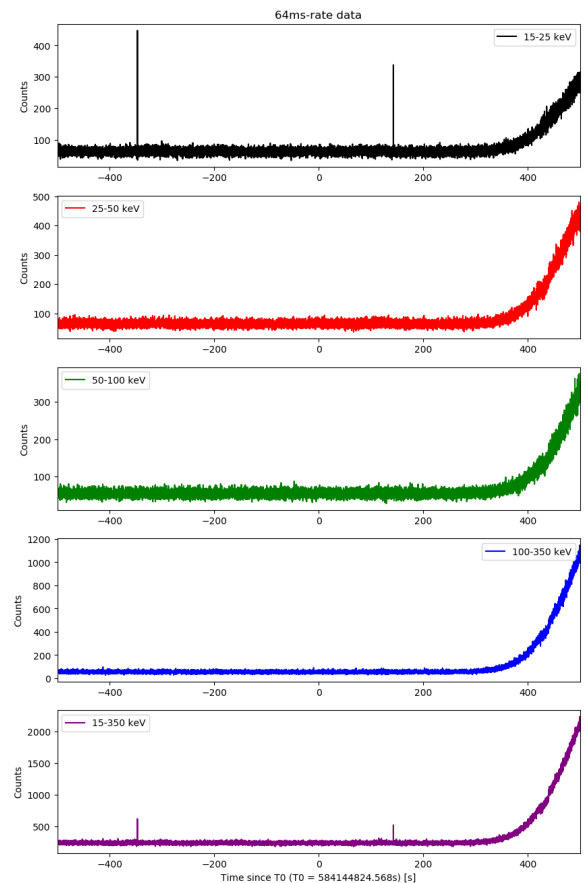
- Third LIGO/Virgo observing run (O3): April 2019 -- March 2020 (commissioning break in October 2019)

Event Name	Date	Time (UTC)	Classification				
GW190408A	04-08-2019	18:18:02	BBH	GW190701A	07-01-2019	20:33:06	BBH
GW190412A	04-12-2019	05:30:44	BBH	GW190706A	07-06-2019	22:26:41	BBH
GW190413A	04-13-2019	05:29:54	not public	GW190707A	07-07-2019	09:33:26	BBH
GW190413B	04-13-2019	13:43:08	not public	GW190708A	07-08-2019	23:24:57	not public
GW190421A	04-21-2019	21:38:56	BBH	GW190719A	07-19-2019	21:55:14	not public
GW190424A	04-24-2019	18:06:48	not public	GW190720A	07-20-2019	00:08:36	BBH
GW190425A	04-25-2019	08:18:05	BNS	GW190727A	07-27-2019	06:03:33	BBH
GW190426A	04-26-2019	15:21:55	BNS/NSBH	GW190728A	07-28-2019	06:45:10	BBH
GW190503A	05-03-2019	18:54:04	BBH	GW190731A	07-31-2019	14:09:36	not public
GW190512A	05-12-2019	18:07:14	BBH	GW190803A	08-03-2019	02:27:10	not public
GW190513A	05-13-2019	20:54:28	BBH	GW190814A	08-14-2019	21:10:39	NSBH
GW190514A	05-14-2019	06:54:16	not public	GW190828A	08-28-2019	06:34:05	BBH
GW190517A	05-17-2019	05:51:01	BBH	GW190828B	08-28-2019	06:55:09	BBH
GW190519A	05-19-2019	15:35:44	BBH	GW190909A	09-09-2019	11:41:49	not public
GW190521A	05-21-2019	03:02:29	BBH	GW190910A	09-10-2019	11:28:07	not public
GW190521B	05-21-2019	07:43:59	BBH	GW190915A	09-15-2019	23:57:02	BBH
GW190527A	05-27-2019	09:20:55	not public	GW190924A	09-24-2019	02:18:46	Mass gap
GW190602A	06-02-2019	17:59:27	BBH	GW190929A	09-29-2019	01:21:49	not public
GW190620A	06-20-2019	03:04:21	not public	GW190930A	09-30-2019	13:35:41	Mass gap
GW190630A	06-30-2019	18:52:05	BBH				

O3a Catalog gravitational-wave events



GW190503: BAT FoV (gradients of red), LVC probability region (light blue), Earth as seen from BAT (yellow).



BAT raw light-curves (time bins of 64 ms, 1 s, and 1.6 s). Calculate average count and standard deviation using the data from ± 100 s from the LVC trigger time; reports any counts > 5 sigma

Estimation of flux limit using the standard deviation calculated from the 1-s binned light curves (GRB simulation code in Lien et al. 2014)

(preliminary)

Number of LVC triggers	39
Number of triggers in BAT FoV ($>10\%$ overlap)	16
Number of BAT >5 sigma detections	0

PROJECT II: SEARCH FOR SPATIAL CORRELATION BETWEEN ICECUBE NEUTRINO EVENTS AND THE FERMI-LAT EXTRAGALACTIC GAMMA-RAY SKY

- The goal: Shed light on the astrophysical neutrino-gamma-ray connection by making use of cross-correlation techniques (2-point cross-correlation function/cross-angular power spectrum) and utilizing information carried by the spatial distribution of gamma-ray and neutrino sources
- Paper in progress: *Search for spatial correlation between IceCube neutrino events and the Fermi-LAT extragalactic gamma-ray sky, M. Negro, M. Crnogorčević, M. Larson, E. Burns, E. Charles, K. Feng, and R. Caputo* (submission expected < 6 months)

Total gamma-ray emission

Resolved sources

Unresolved emission (~20%)

not negligible fraction!

Resolved gamma-ray srcs and neutrinos

Galactic

Super Novae remnants
young pulsar wind nebulae
Galactic plane

~20% neutrino flux

Extragalactic

blazars from the 3LAC
Star Forming Galaxies
Active galactic nuclei (mAGN)

<20% neutrino flux

~50% neutrino flux

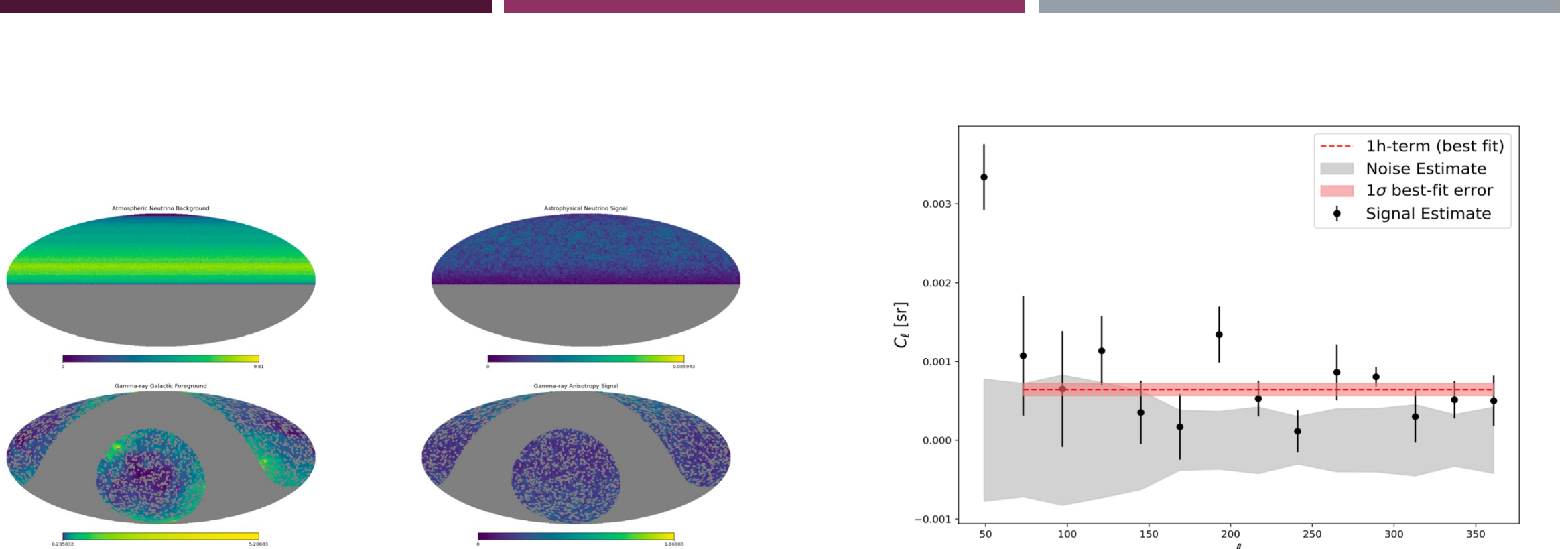


Fig. 7.— All-sky expected counts maps, in counts per $0.458^{\circ 2}$ pixel (HEALPix nside=128) for simulated atmospheric neutrino (top left), astrophysical neutrino (top right), galactic gamma-ray foreground (bottom left) and gamma-ray signal (bottom right). The grey regions mark the masked pixels. See e.g. (Fang et al. 2020) for details on mask choice.

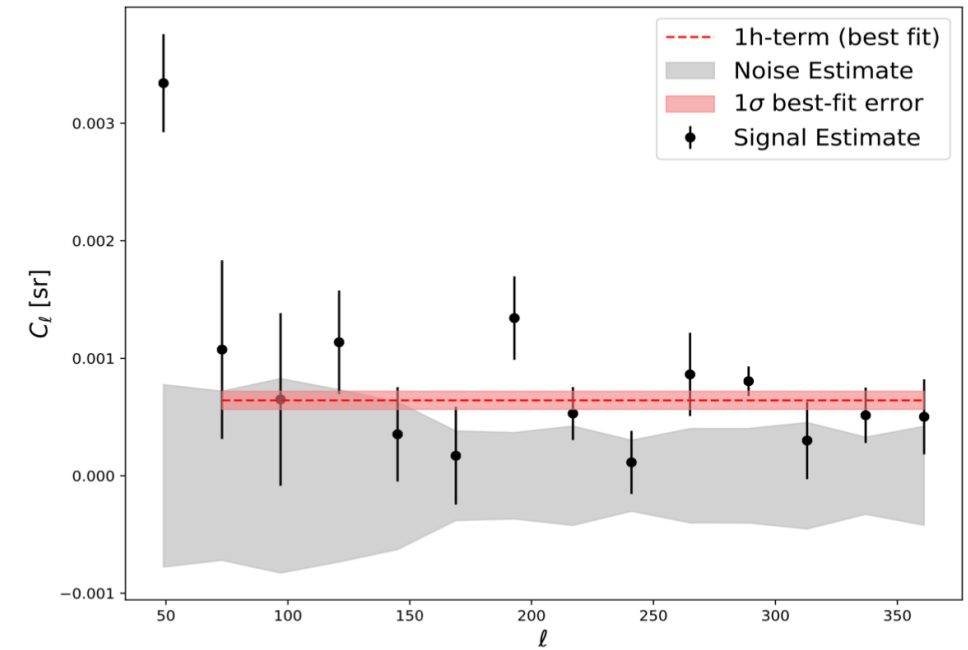


Fig. 8.— Comparison of expected signal and noise levels for cross-correlation of simulated 10-year neutrino data with gamma-ray data. The red dashed line and the red shaded band are the best fit and the relative 1σ error for a 1halo-term component, as described in the halo model formalism (Cooray & Sheth 2002).

This approach will be advantageous for several aspects:

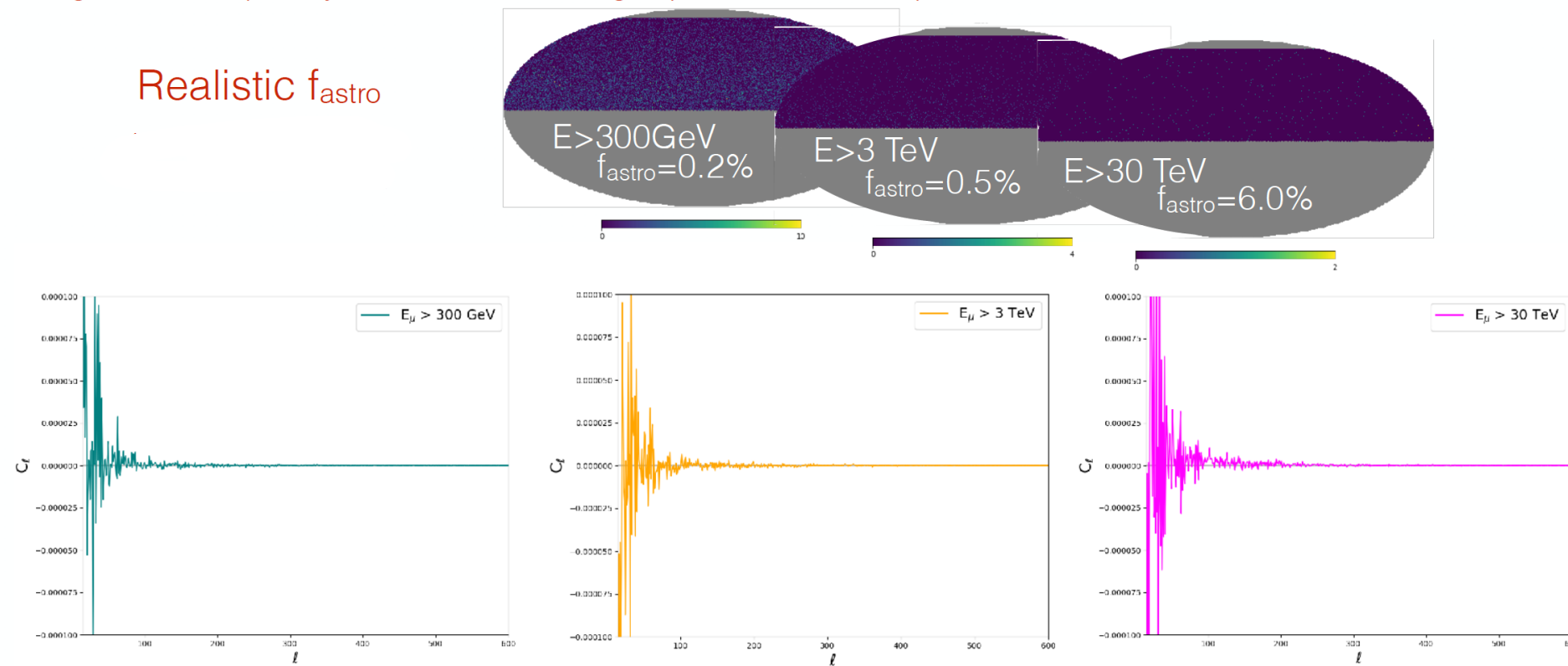
1. it is sensitive also to **faint gamma-ray sources** that populate the sub-threshold regime
2. it includes information given by the relative positions of neutrinos, namely their global **spatial distribution**, in addition to the localization of each single event.
3. There are less uncertainties related to **mis-modeling of gamma-ray background** (galactic large scale structures are not expected to correlate with "point-like" neutrino signal).
4. There is the possibility to **partially mask** the sky (to exclude particularly high background regions or parts of the sky with poor angular resolution; also, this would allow interesting tests covering different type of resolved sources and studying the signal variations)

PROJECT II: SEARCH FOR SPATIAL CORRELATION BETWEEN ICECUBE NEUTRINO EVENTS AND THE FERMI-LAT EXTRAGALACTIC GAMMA-RAY SKY

Comparisons with simulations (details in backup slides):

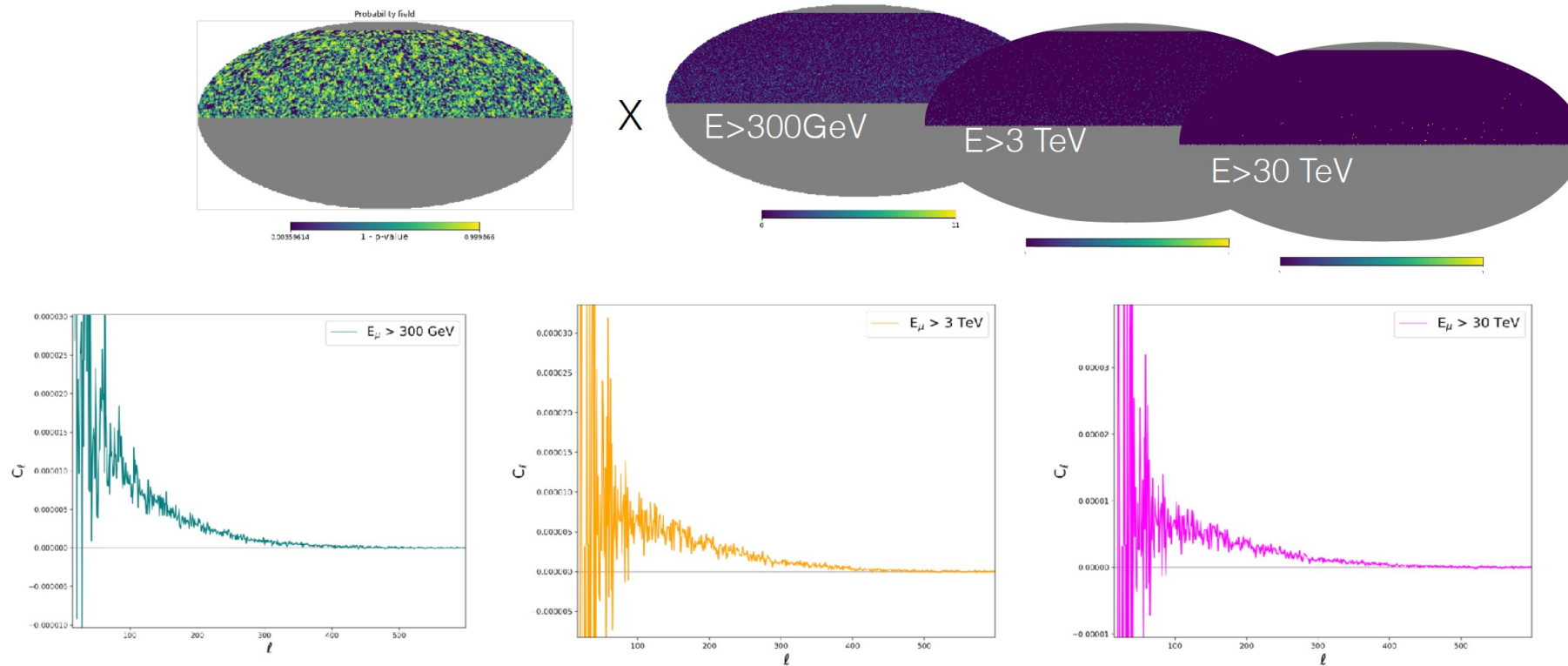
Signal events spatially distributed according to p-value source map

Realistic f_{astro}



PROJECT II: SEARCH FOR SPATIAL CORRELATION BETWEEN ICECUBE NEUTRINO EVENTS AND THE FERMI-LAT EXTRAGALACTIC GAMMA-RAY SKY

Cross-correlation p-value X IC events (3yrs data release)



Successful outcomes:

- 1) A significant positive cross-correlation signal is found with the total (resolved and unresolved) extra-galactic gamma-ray sky.

This would be the definitive proof that the neutrino background is indeed associated to gamma sources. Furthermore, if the signal amplitude varies (decrease) when the contribution of one particular class of resolved sources, e.g. BL-LACs, is cut away (by applying a mask) it would directly indicate that those sources are effectively powering the neutrino flux that we observe.

- 2) A significant positive cross-correlation signal is found with the unresolved extra-galactic gamma-ray sky and does not vary when adding the resolved ones.

Now, if the signal does not vary whether or not the resolved sources are masked, the neutrino background is associated to the same sub-threshold sources which produce the intensity fluctuations in the UGRB. In this case it will be possible to infer (through proper modeling) the most effective class(es) of sources that can simultaneously produce the observed neutrino background and the anisotropy that we observe in the UGRB (mAGNs, ...).

- 3) A null- signal is found.

This might result for two reasons, both of which are still interesting: 1) the neutrino signal does not truly correlate with gamma-ray sources, meaning that its origin must be searched in "gamma-blind" sources, driving the focus of the search to other bands of the electromagnetic spectrum; 2) the neutrino events are associated with particular gamma-ray source populations with a very low intrinsic anisotropy, whose concomitant emission results in a too diffuse glow to contribute to the measured fluctuations: this is the case of star forming galaxies.

Less successful outcomes of this investigation:

- 1) Non-significant positive signal

Poor statistics; not really informative results... but could still be useful to motivate upgrades of the experiments / future missions



BACK-UP SLIDES

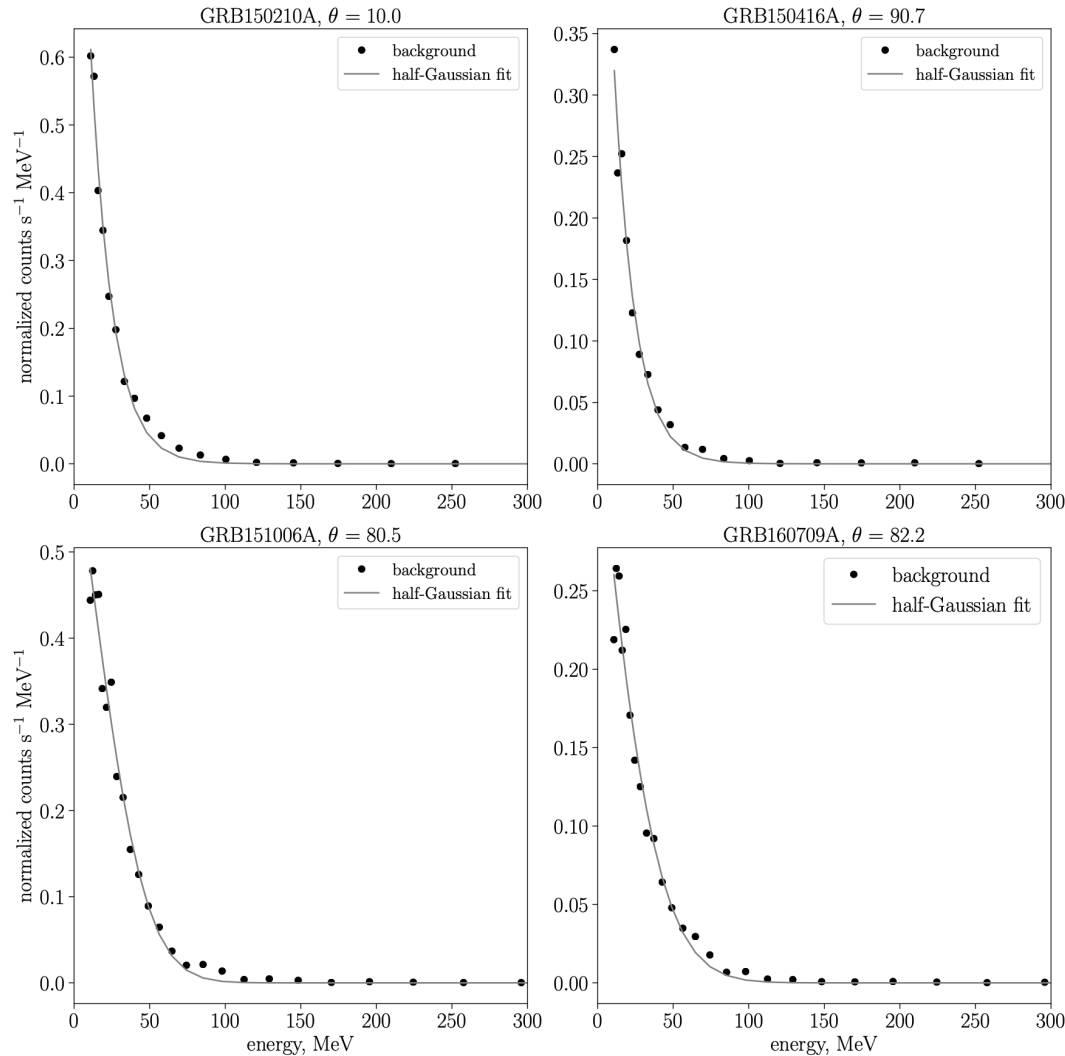




CHAPTER I: SENSITIVITY ANALYSIS



I. FERMI-LLE: SENSITIVITY TESTING: ANALYSIS AND RESULTS



Model backgrounds from the considered LLE-detected GRBs with no redshift.

Find the min, max, and average background counts levels.

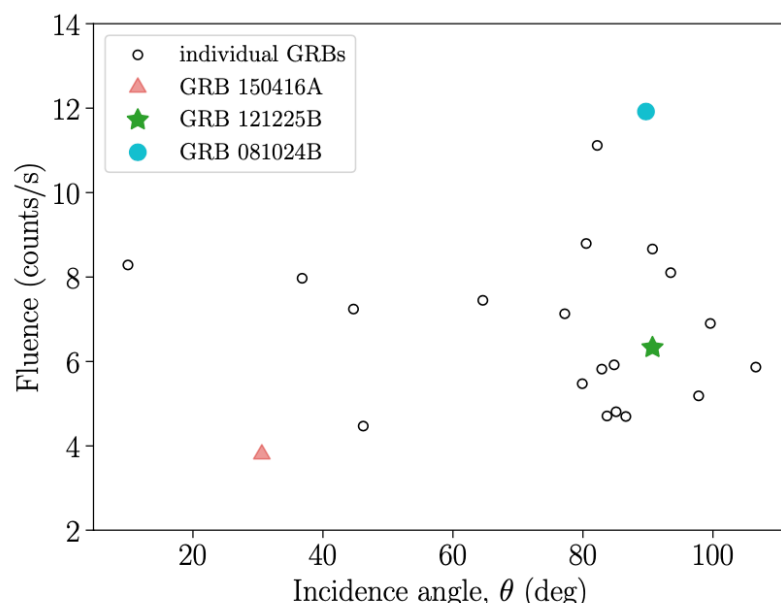
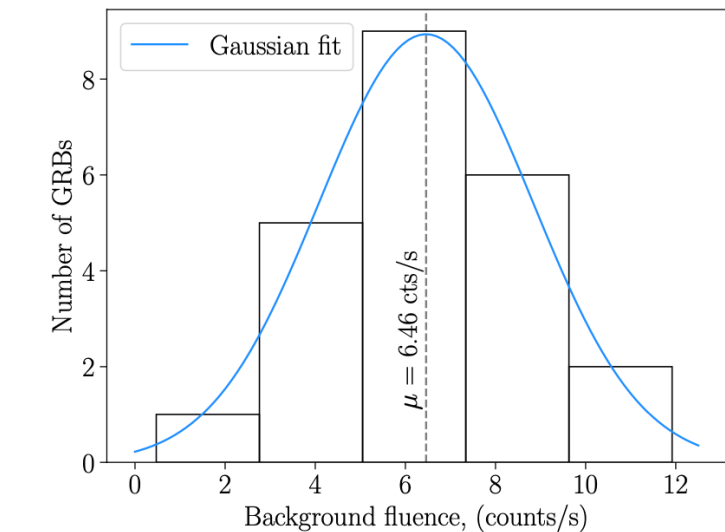
Produce ALP signal normalized by a value from the normalization grid for 10- and 18- solar-mass progenitors.

Produce 2000 realizations of the background+ALP spectrum and their corresponding (GRB) response functions (XSPEC fakeit function.)

Fit the ALP and the “background-only” (or zero) model. Apply Wilks’ Theorem and LLR test to find for which normalization ALP model is preferred.

Find the coupling-distance parameter space for the that normalization.

I. FERMI-LLE: SENSITIVITY TESTING: ANALYSIS AND RESULTS



Model backgrounds from the considered LLE-detected GRBs with no redshift.

Find the min, max, and median background counts levels.

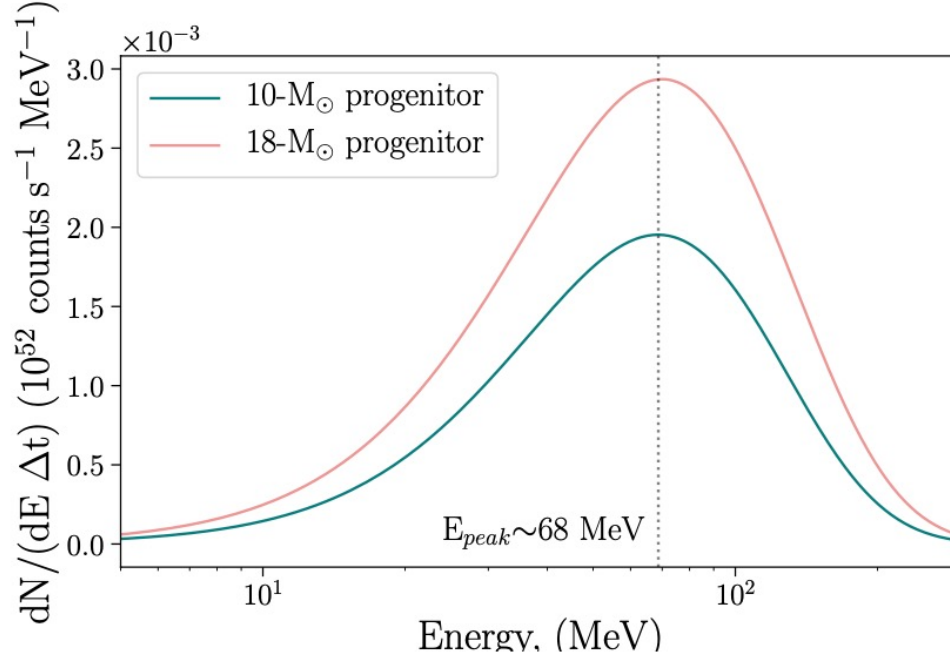
Produce ALP signal normalized by a value from the normalization grid for 10- and 18- solar-mass progenitors.

Produce 2000 realizations of the background+ALP spectrum and their corresponding (GRB) response functions (XSPEC fakeit function.)

Fit the ALP and the “background-only” (or zero) model. Apply Wilks’ Theorem and LLR test to find for which normalization ALP model is preferred.

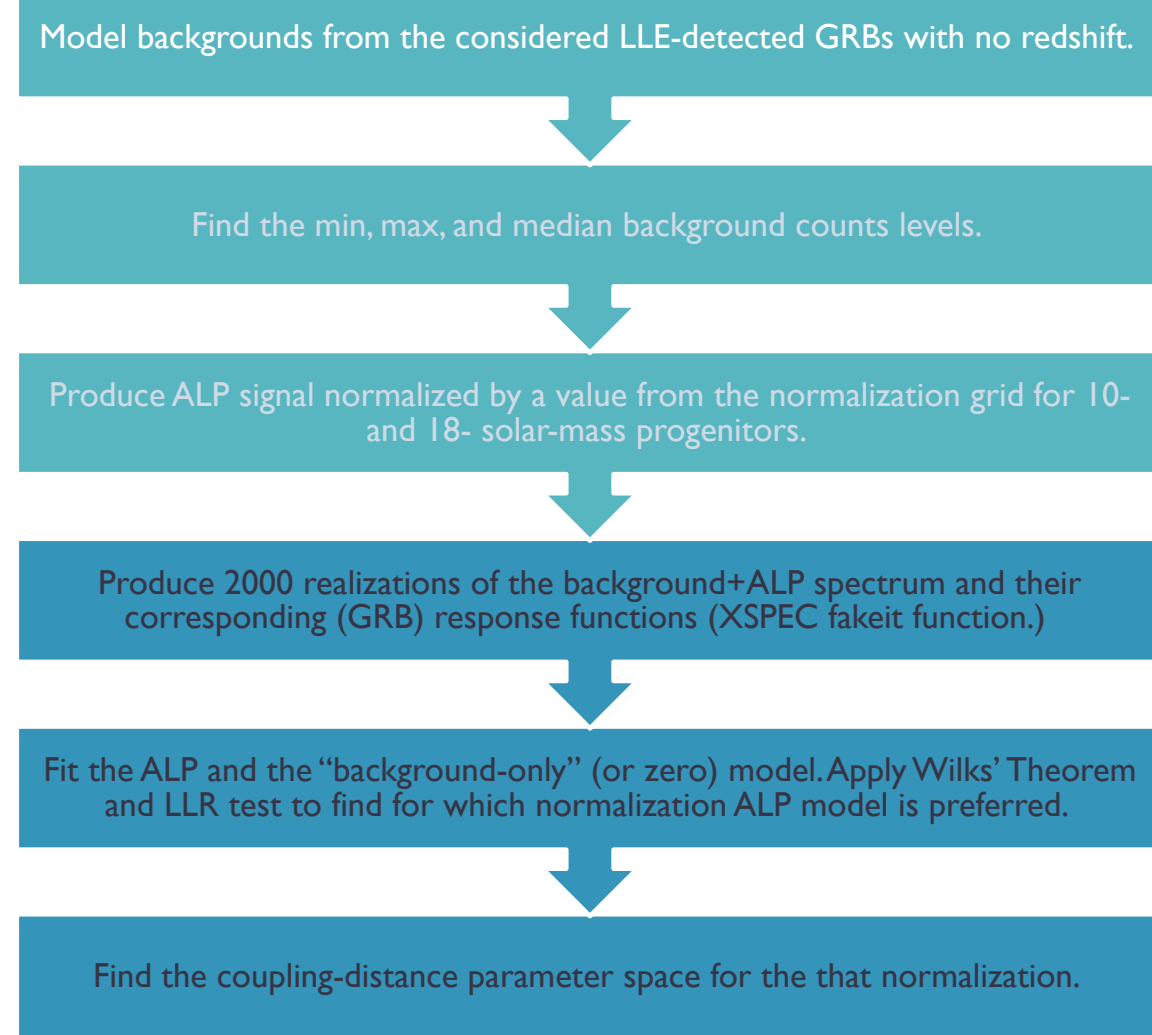
Find the coupling-distance parameter space for the that normalization.

I. FERMI-LLE: SENSITIVITY TESTING: ANALYSIS AND RESULTS

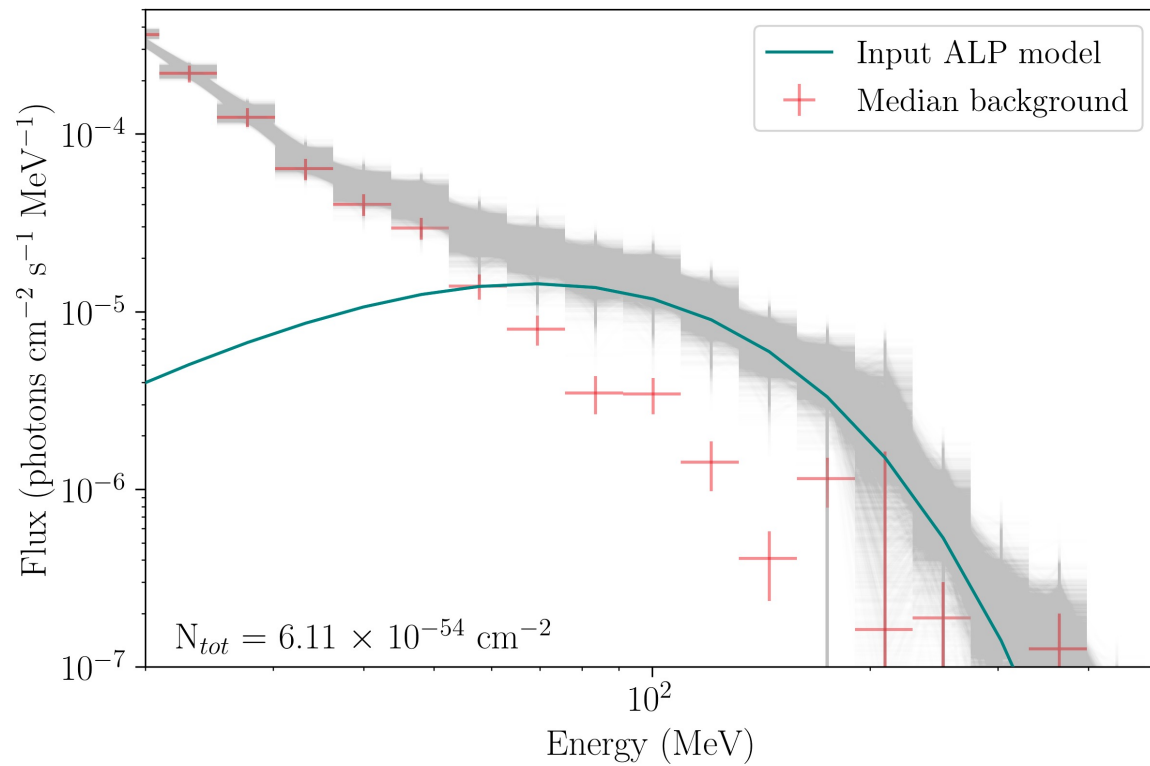


- scaled by 30 normalization values logarithmically distributed between $N_0 = 8.4 \times 10^{-60}$ and $8.4 \times 10^{-50} \text{ cm}^{-2}$

$$N_0 \propto \frac{g_{a\gamma\gamma}^4}{d^2}$$



I. FERMI-LLE: SENSITIVITY TESTING: ANALYSIS AND RESULTS



Model backgrounds from the considered LLE-detected GRBs with no redshift.

Find the min, max, and median background counts levels.

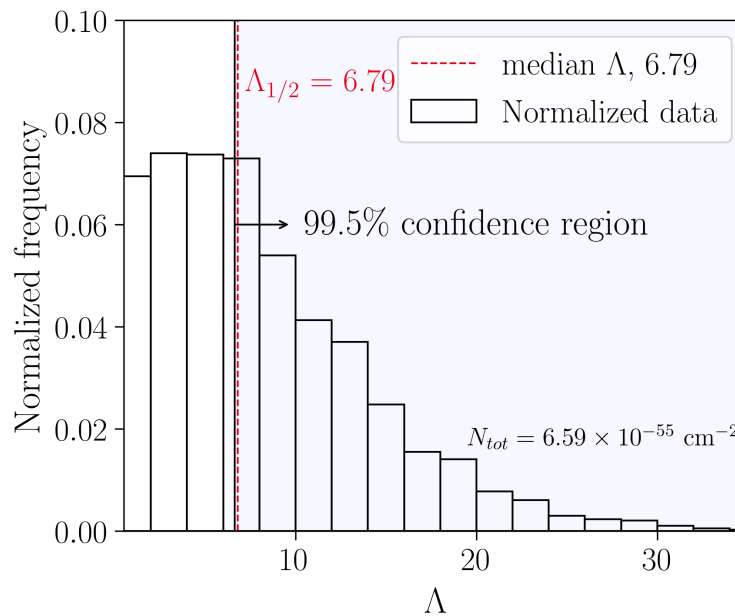
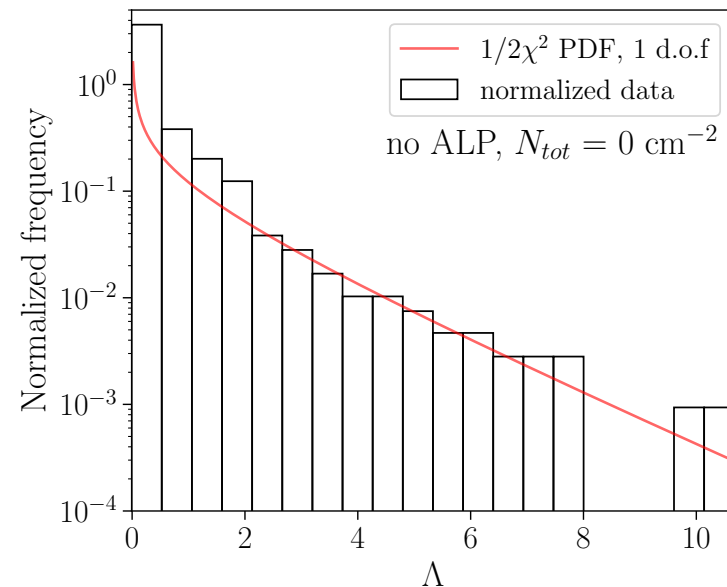
Produce ALP signal normalized by a value from the normalization grid for 10- and 18- solar-mass progenitors.

Produce 2000 realizations of the background+ALP spectrum and their corresponding (GRB) response functions (XSPEC fakeit function.)

Fit the ALP and the “background-only” (or zero) model. Apply Wilks’ Theorem and LLR test to find for which normalization ALP model is preferred.

Find the coupling-distance parameter space for the that normalization.

I. FERMI-LLE: SENSITIVITY TESTING: ANALYSIS AND RESULTS



Model backgrounds from the considered LLE-detected GRBs with no redshift.

Find the min, max, and median background counts levels.

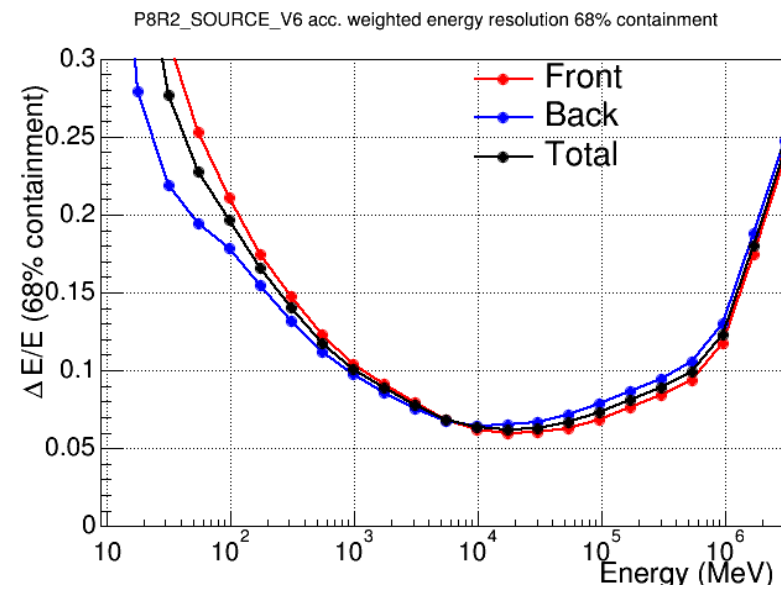
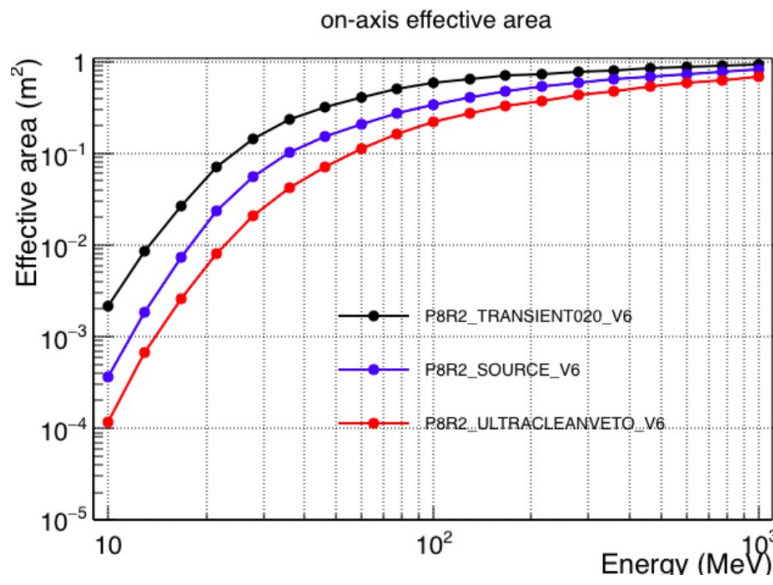
Produce ALP signal normalized by a value from the normalization grid for 10- and 18- solar-mass progenitors.

Produce 2000 realizations of the background+ALP spectrum and their corresponding (GRB) response functions (XSPEC fakeit function.)

Fit the ALP and the “background-only” (or zero) model. Apply Wilks’ Theorem and LLR test to find for which normalization ALP model is preferred.

Find the coupling-distance parameter space for the that normalization.

LAT SENSITIVITY + EFFECTIVE AREA

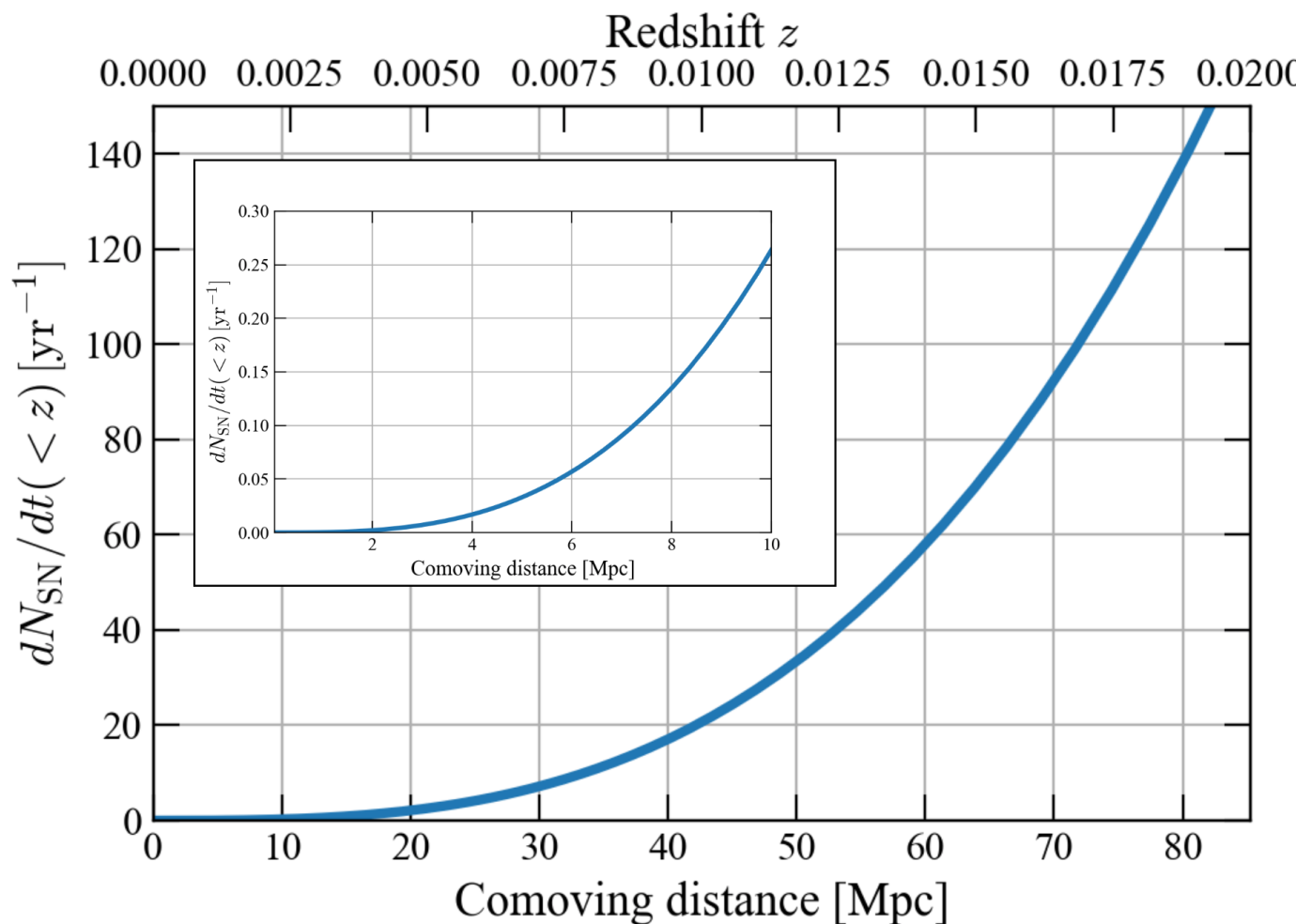




CHAPTER I: OPTICAL LIGHTCURVE ANALYSIS

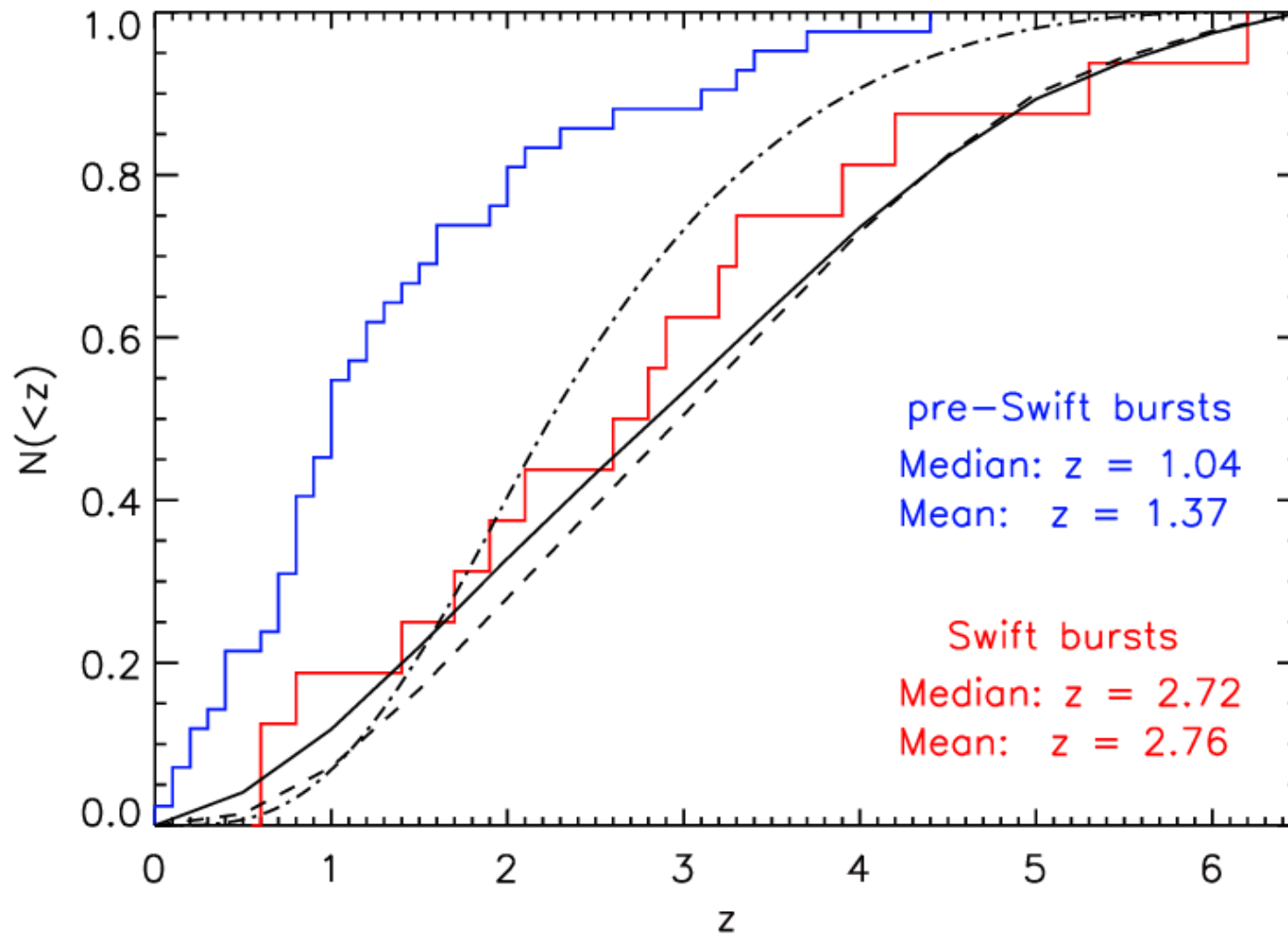


SN RATE AS A FUNCTION OF COMOVING DISTANCE



- SN Rate: $\sim 150 \text{ yr}^{-1}$ up to $z = 0.02$ (following Lien et al. 2009 with Salpeter IMF from Baldry et al. 2003 and cosmic SFR from Hopkins et al. 2006)
- Likely underestimated local SN rate by a factor of few (Ando et al. 2005, Kistler et al. 2013)
- No neutrino signal with the current generation of the neutrino detectors (Kistler et al. 2011)

GRB # AS A FUNCTION OF DISTANCE (CUMULATIVE FRACTION)



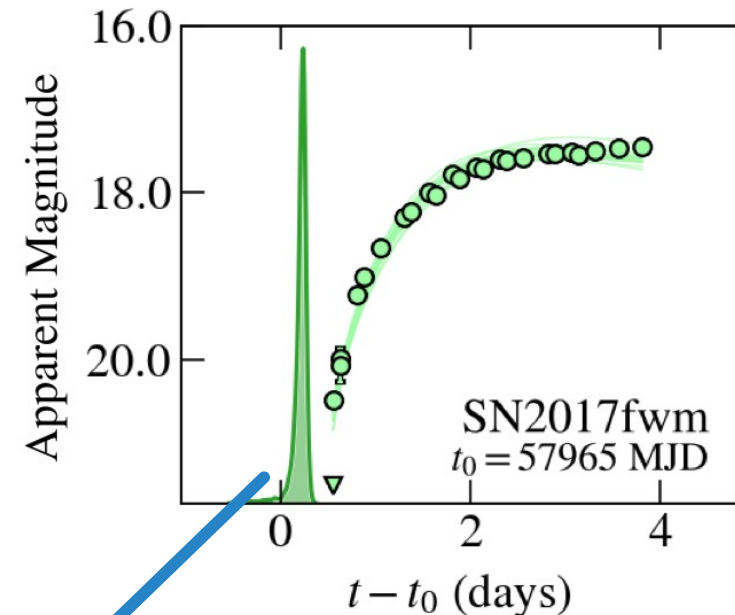
II.

PROPOSED ANALYSIS AND EXPECTED RESULTS

I. Determination of the collapse time for a supernova sample

[Meyer et al. 2020]

- Using the MOSFiT package to fit the lightcurves and estimating Bayesian posteriors and evidences [Guillochon et al. 2018]
- Model for the SN: engine (radioactive decay of ^{56}Ni and ^{56}Co or exponential power law) + Diffusion + Blackbody SED [Nicholl et al. 2018, Villar et al. 2017]



Marginal posterior for the explosion time

II.

METHOD

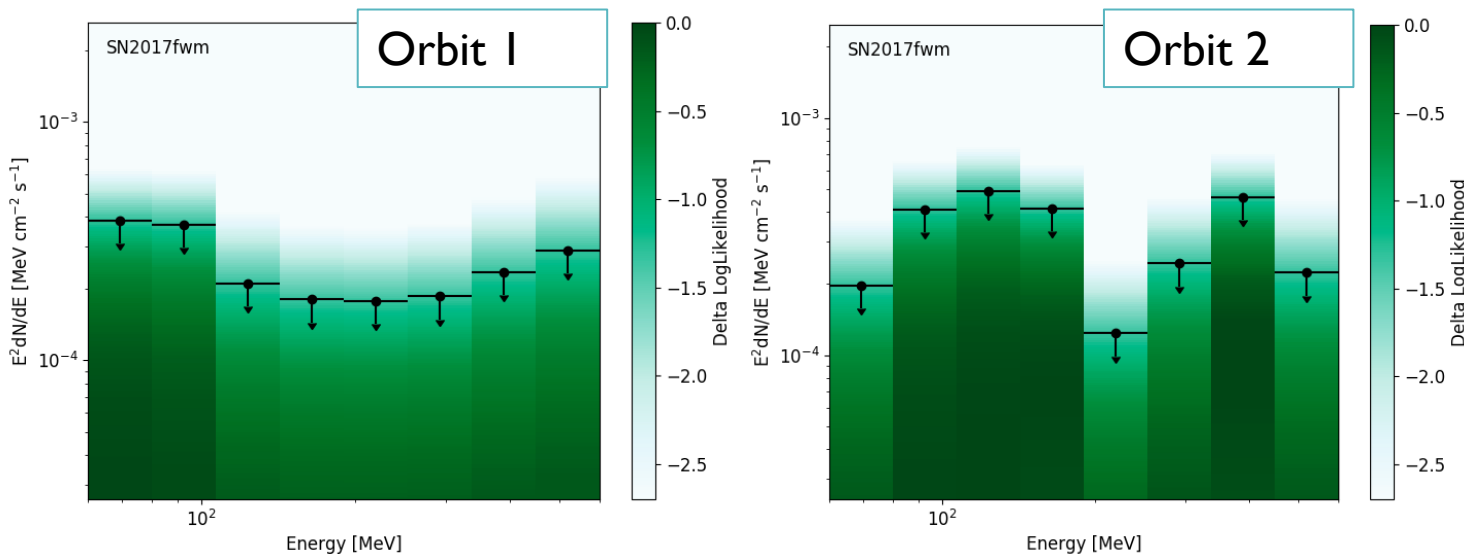
III. *Fermi* LAT Selection Criteria

- Event class: P8R3 SOURCE
- Energy range: 60 – 600 MeV
- Binning 8 log energy bins, 0.5° per pixel
- Time range: ± 30 days around discovery date
- ROI size: $20^\circ \times 20^\circ$
- Zenith angle $< 80^\circ$

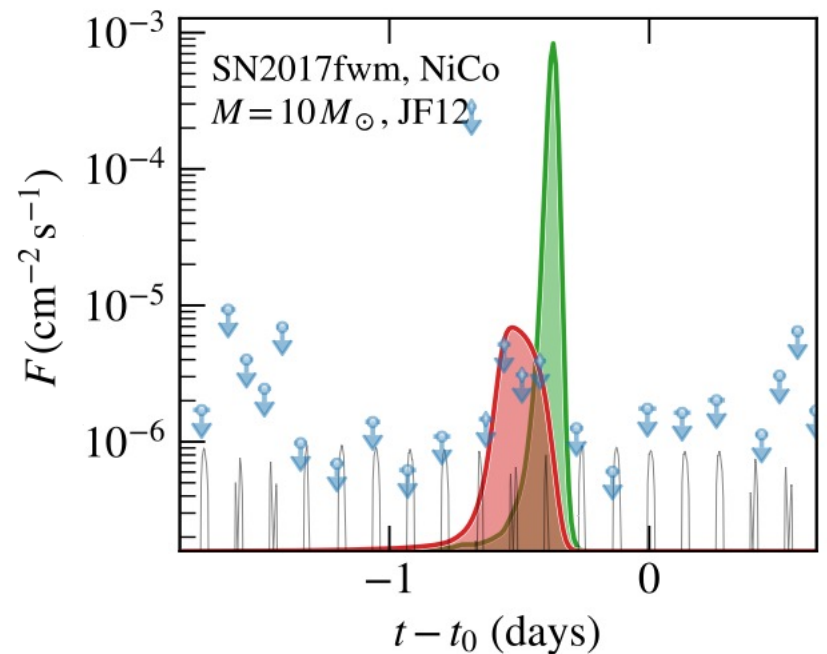
II. METHOD

III. Fermi LAT Analysis procedure

1. Add a SN to the ROI model assuming ALP model
2. Calculate gamma-ray light curve ± 30 days around SN discovery date with one time bin per orbit ($\sim 2 \times 30 \times 24 / 1.5 = 960$ orbits)
3. Derive SED and log-likelihood curve in each energy bin

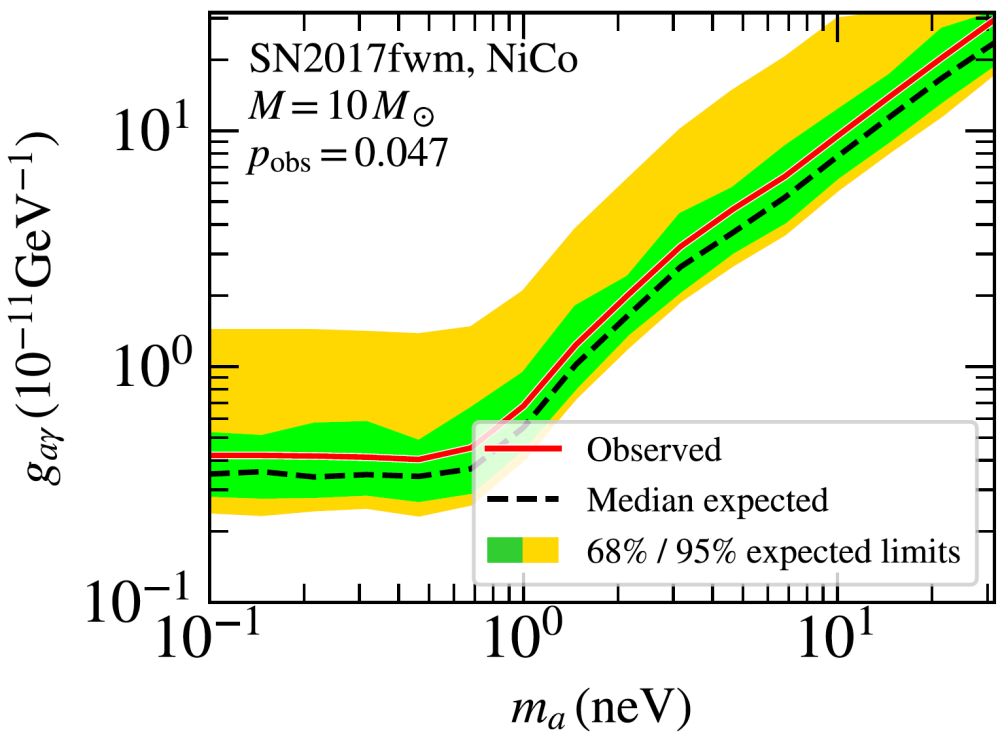


Plots adapted from M. Meyer et al. 2020



II. METHOD

III. Limits for one supernova, TS = 0 → Limit!



Combining
Likelihoods:

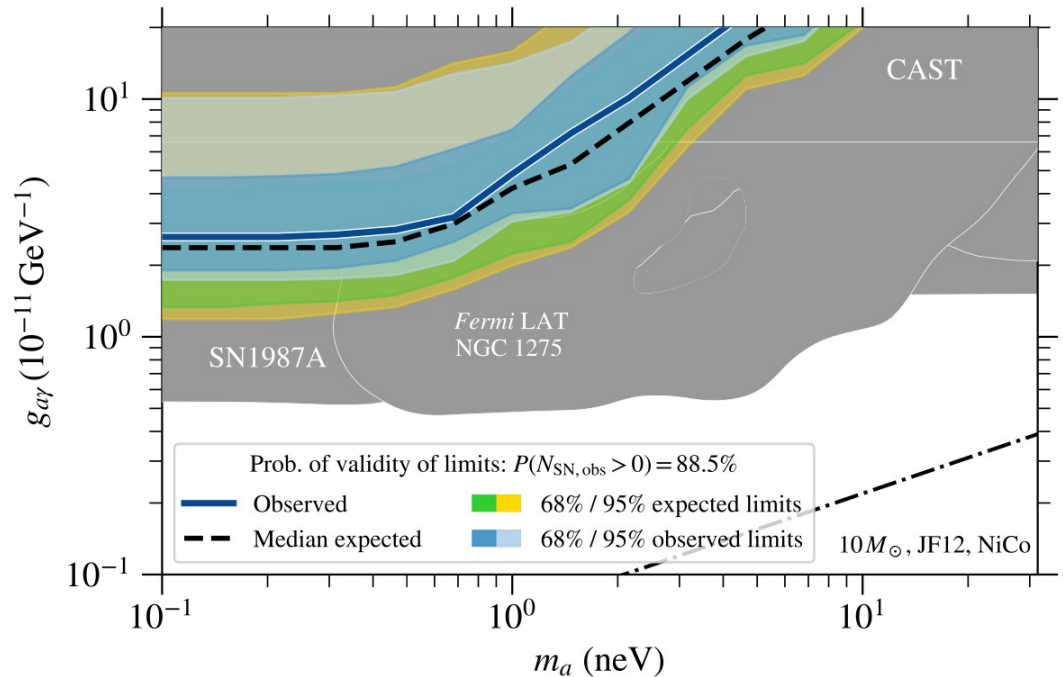
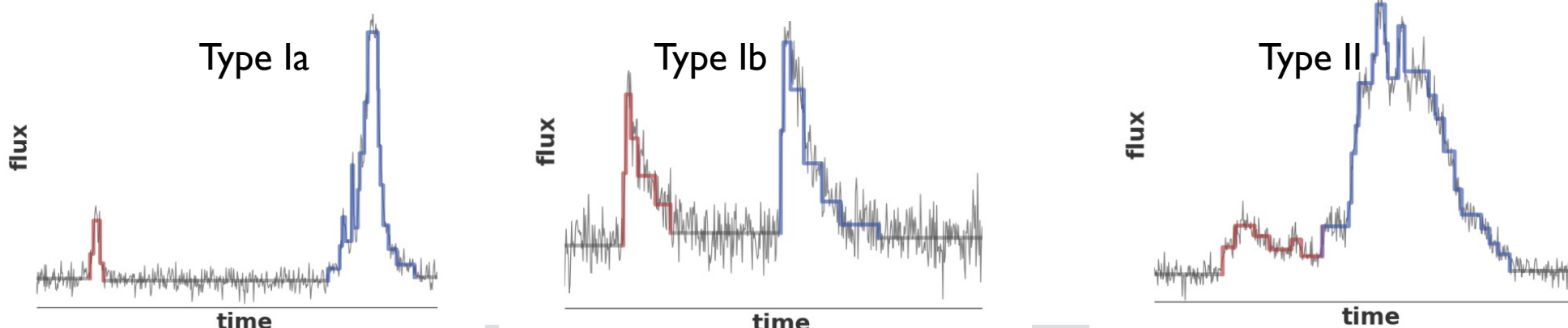


FIG. 2. Combined observed (blue shaded regions) and expected limits (green and yellow regions) from stacking the likelihoods of different SNe under the assumption that at least one SN was observed during the time of the core collapse. The median observed limit is shown as a blue solid line, whereas the median expected limit is shown as a dashed black line. Grey shaded regions show the parameter space excluded by other experiments [10, 50, 63–65]. Below the black dash-dotted line, ALPs could constitute the entire dark matter [5].

III. METHOD

- Sort out the precursor emission into different subcategories:
 - Type I: Flux returns to background levels with the "silent" interval at least as long as the main episode
 - Type Ia: The flux of the precursor emission is <50% of the main emission flux
 - Type Ib (Type III): The flux of the precursor emission is >50% of the main emission flux
 - Type II: No evening out with the background, double peaked
- Adapt the Bayesian block algorithm from the *Fermi* Team to all GBM GRBs to identify those with a precursor
- Once a sample of the GBM GRBs has been selected, apply the similar upper-limit analysis as for the CCSNe.



BACK-UP: IC X FERMI

Autocorrelation

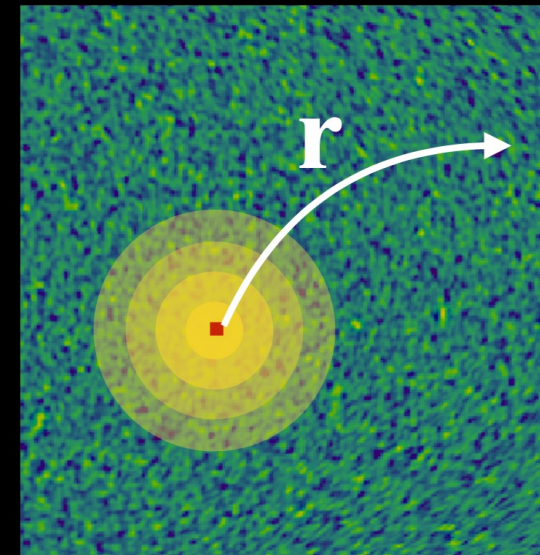
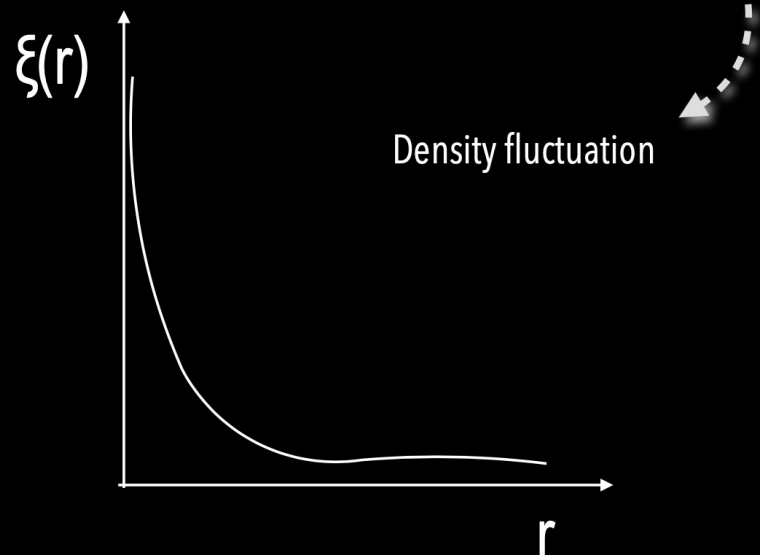
$$dP = n [1 + \xi(\mathbf{r})] dV$$

Measures the excess probability, above the expectation from a random distribution, of finding an over density in a volume dV at a separation \mathbf{r} from another

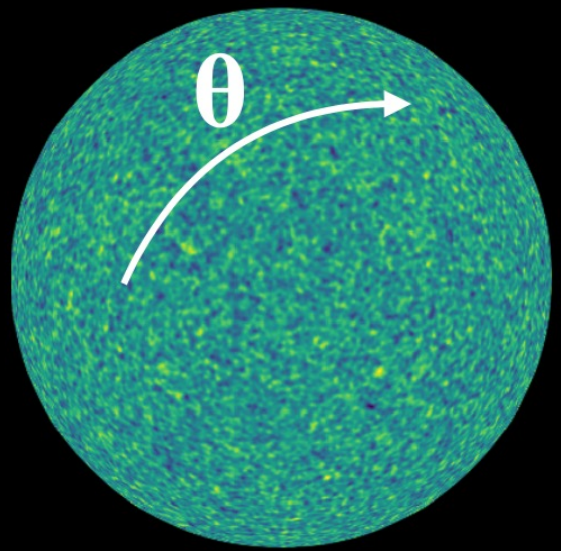
$$\xi(\mathbf{r}) = \langle \delta(\mathbf{x}) \delta(\mathbf{x} + \mathbf{r}) \rangle$$

2-point autocorrelation function (ACF)

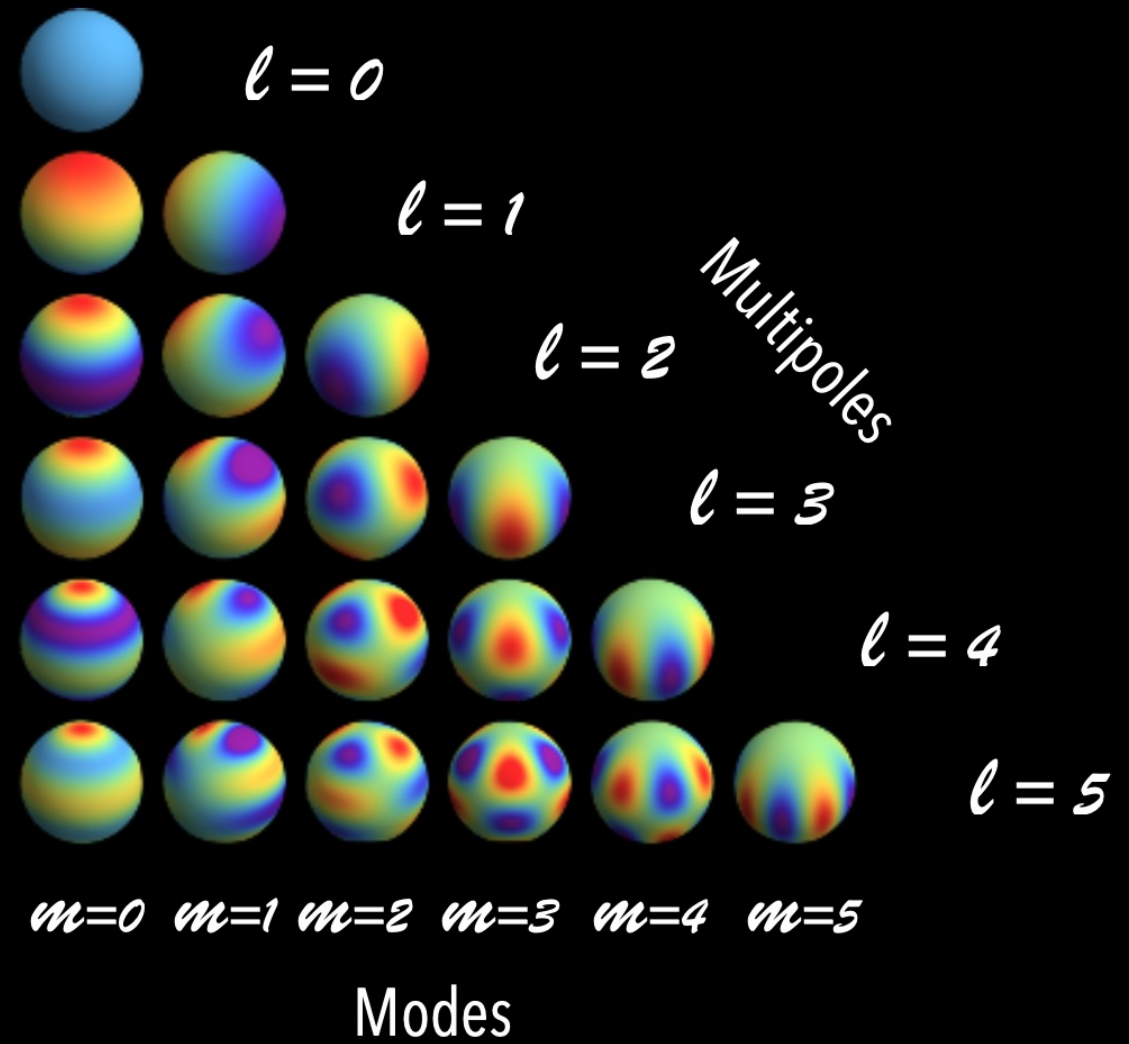
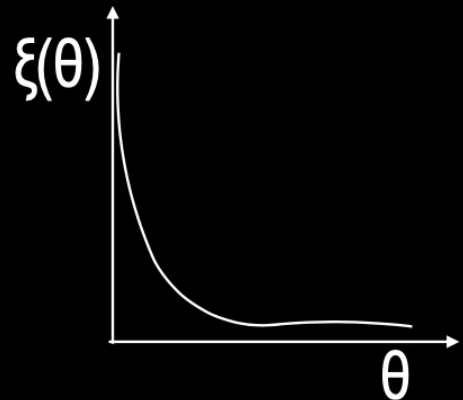
$$\delta(\mathbf{x}) = \frac{n(\mathbf{x})}{\langle n \rangle} - 1$$



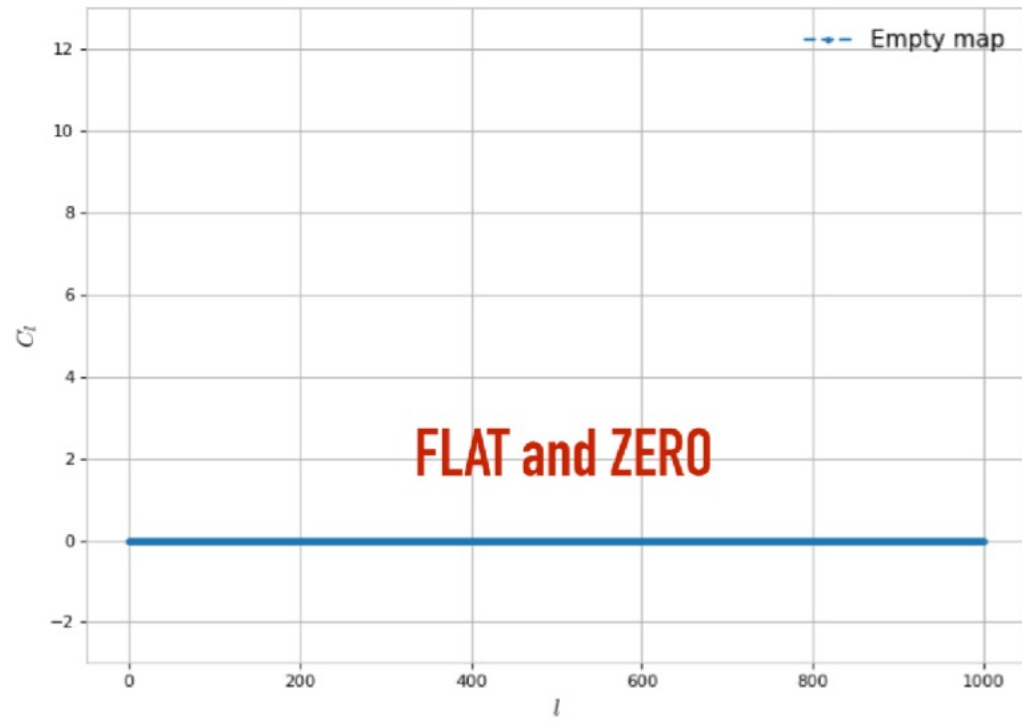
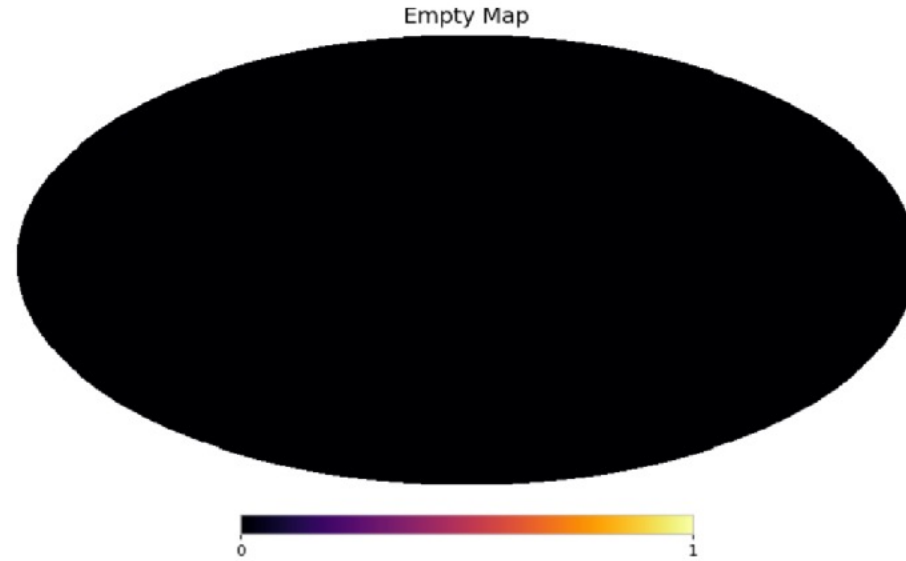
Anisotropy on a sphere



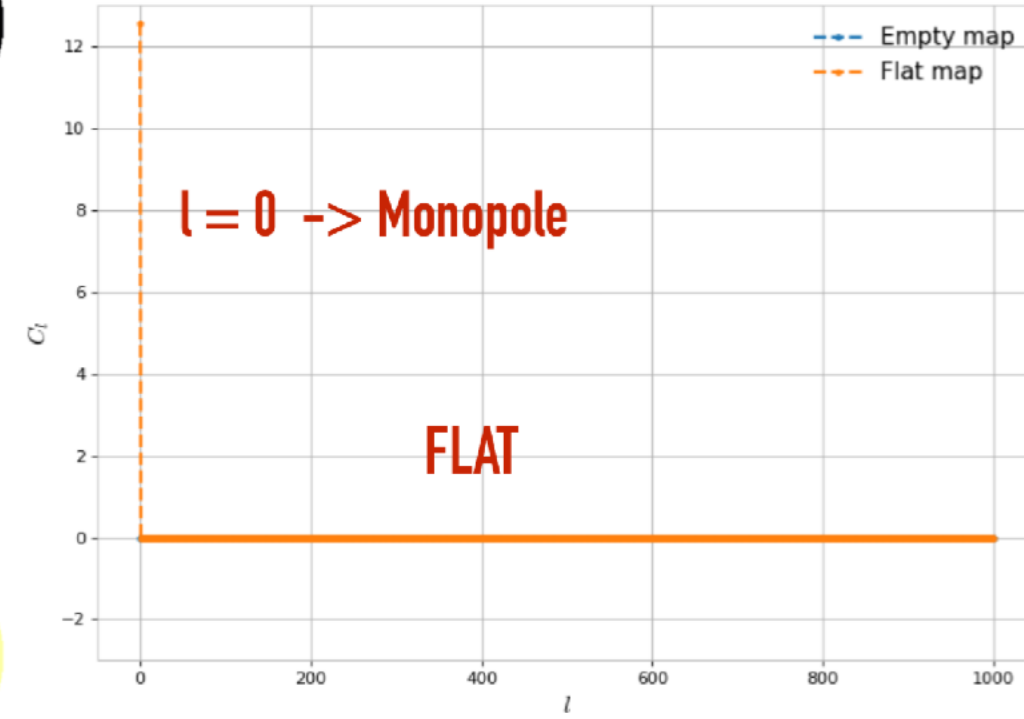
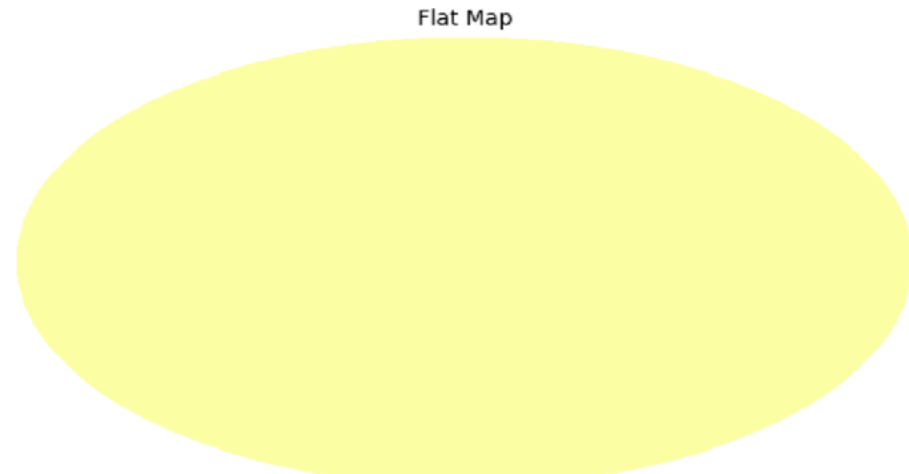
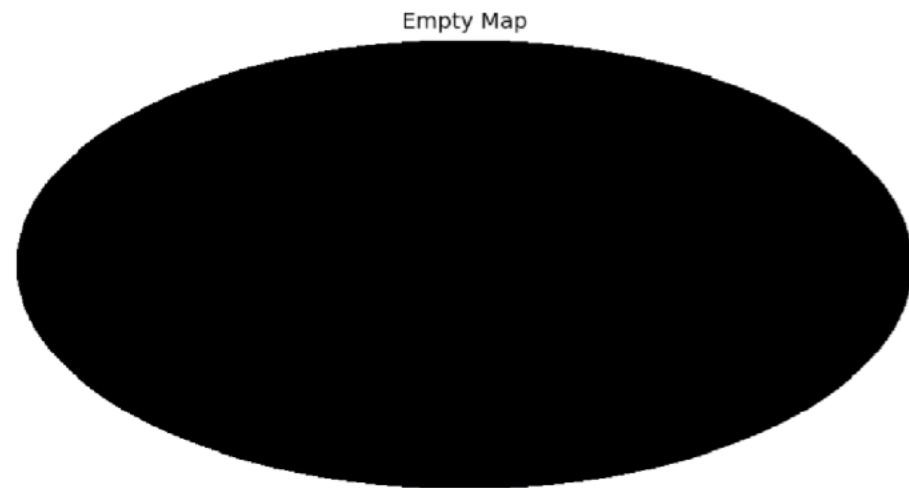
Physical space



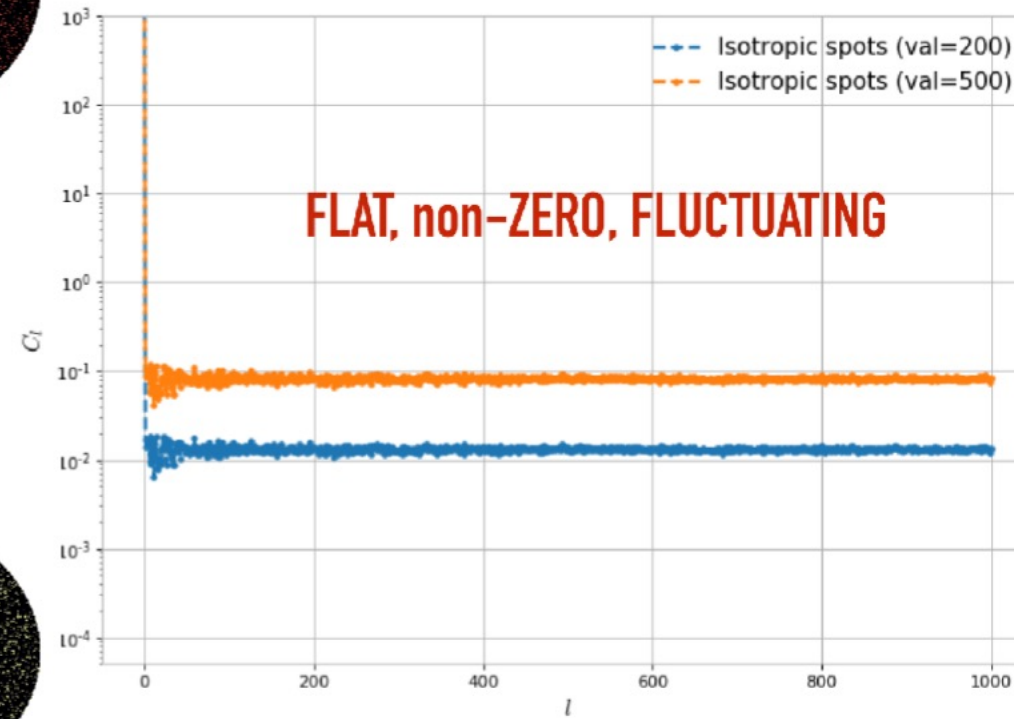
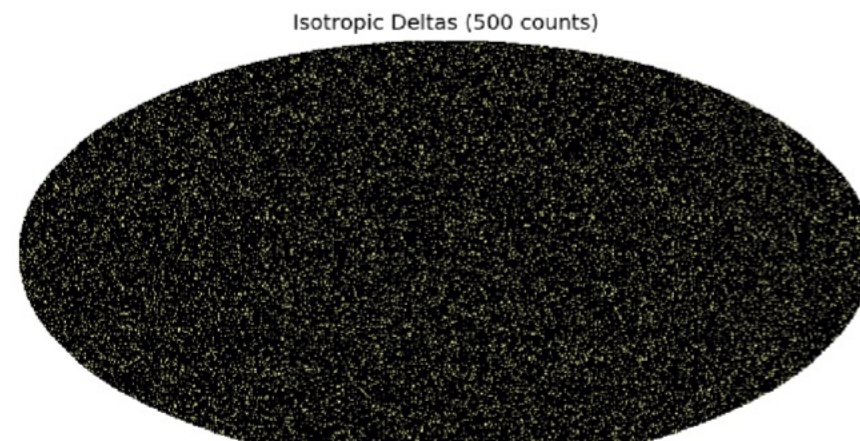
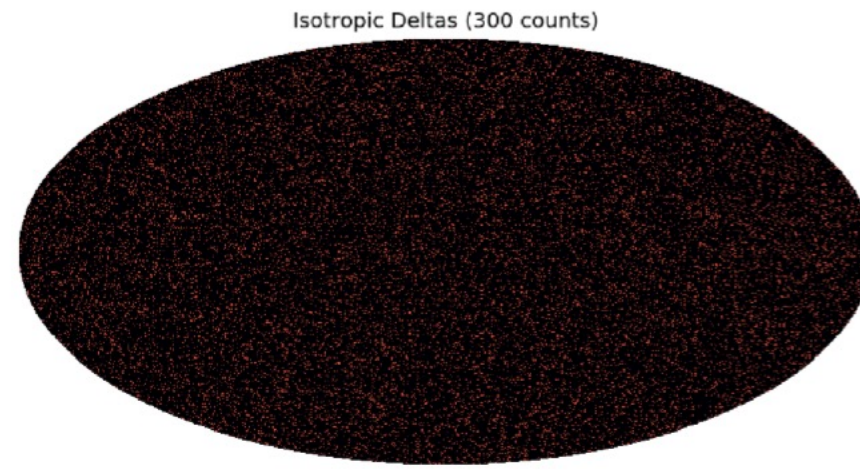
Some simple examples:



1- Intro To APS

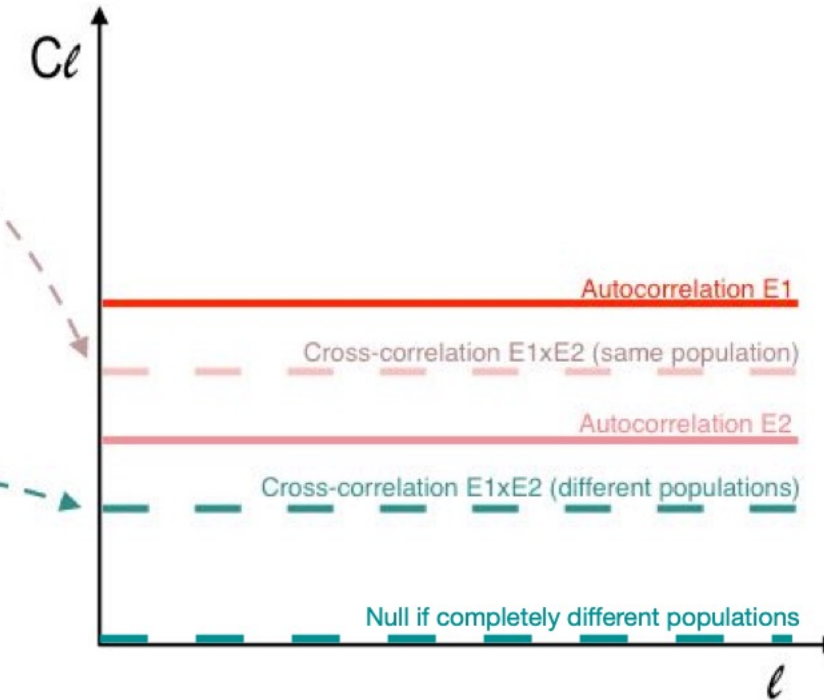
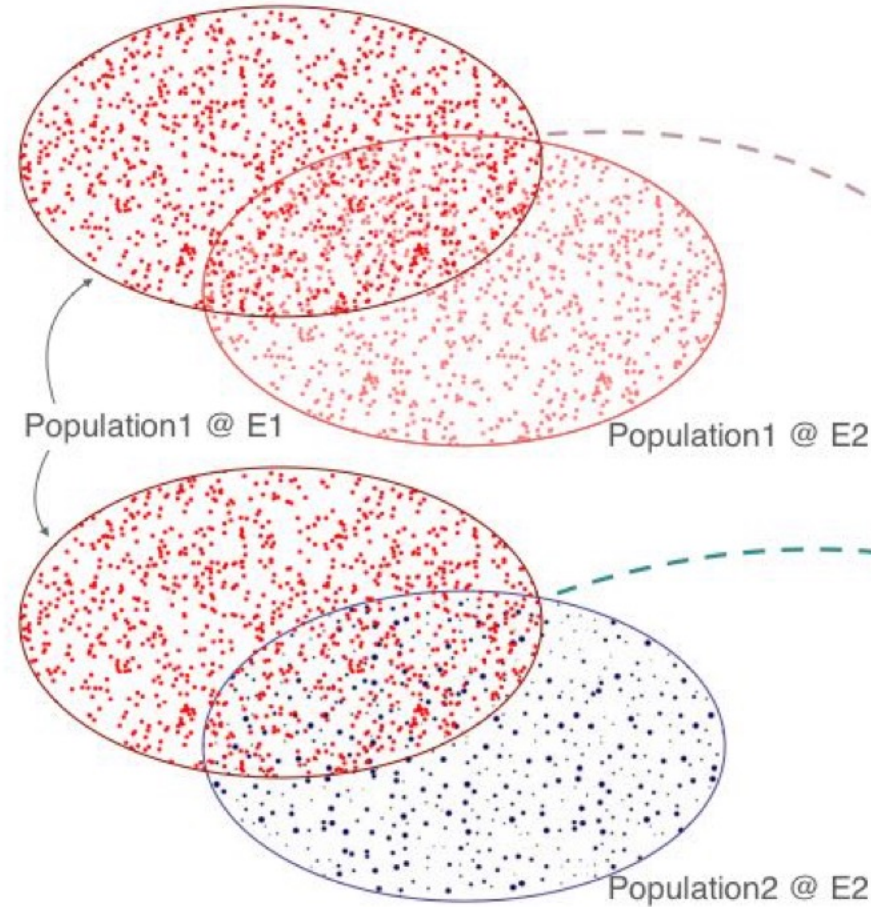


1- Intro To APS

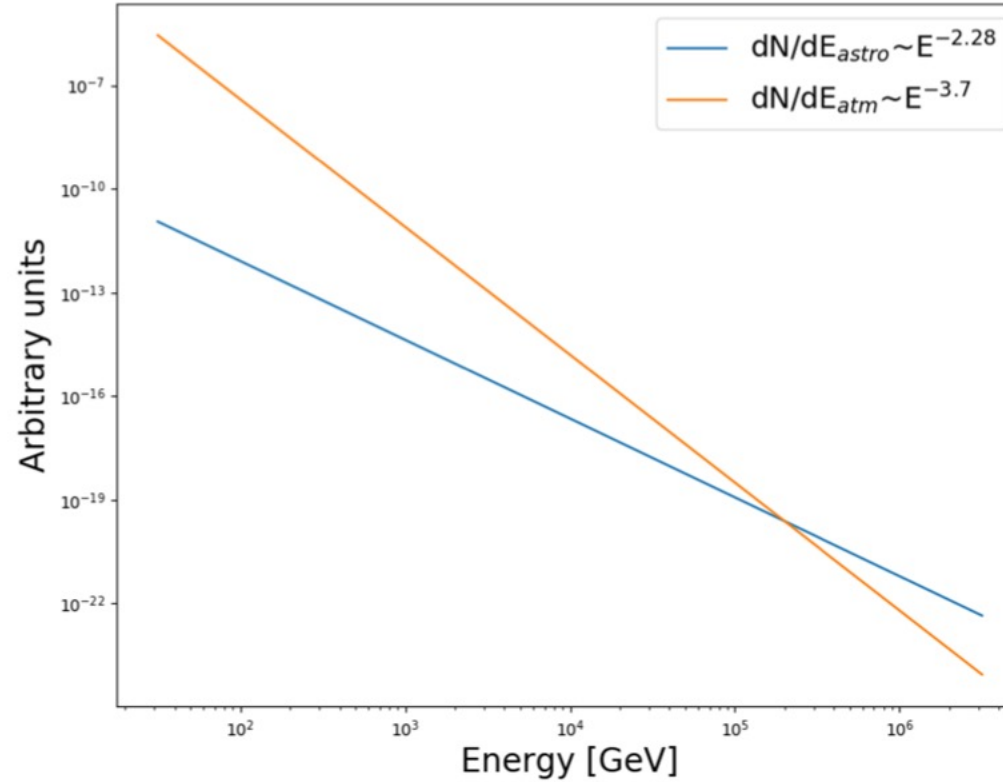


1- Intro To APS

Cross-correlating two maps hosting the same or different source distributions



f_{astro} as a function of E

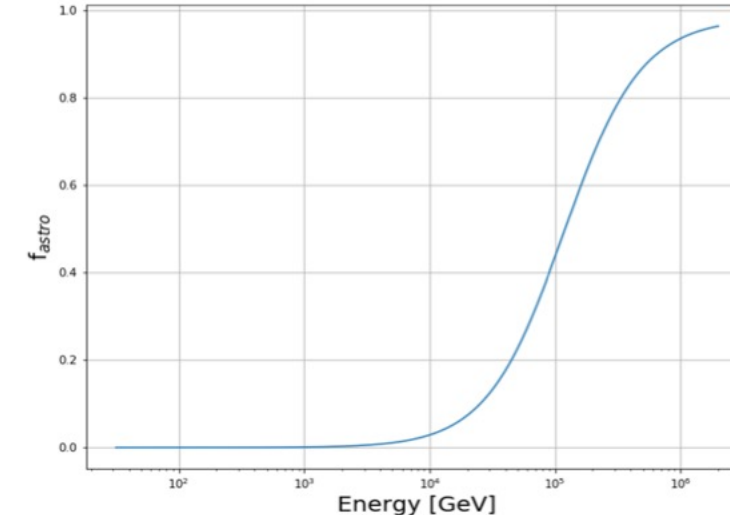


In the plot :

$$dN/dE_{\text{astro}}(2\text{e}5) = dN/dE_{\text{atm}}(2\text{e}5)$$

As in <https://pos.sissa.it/358/1017/pdf>

ATT: for the simulations we only care about the spectral slope (both curves are normalized to one and the statistics is given by the energy distribution of real data).





GENERAL



INTRODUCTION: THE DIFFERENCE BETWEEN AXIONS AND ALPs

- QCD axion: $m_a \sim 1/f_a$, where f_a is the energy breaking scale
- Axionlike particles: m_a and f_a are **independent parameters**
- Predicted in several **extensions** of the standard model (Majoron, Familon, String Theory...) [see Jaeckel & Ringwald 2010 for a review)
- **Do not solve** the strong CP problem

PRIMAKOFF RATE

2.2 Primakoff rate

ALPs coupled to the electromagnetic radiation as in Eq. (1.1) are produced in the stellar medium primarily through the Primakoff process [31], in which thermal photons are converted into ALPs in the electrostatic field of ions, electrons and protons.

Using the Heaviside–Lorentz convention for electromagnetism, the Primakoff conversion rate per unit time of photons into pseudoscalars is given by the following expression,

$$\Gamma = \frac{g_{a\gamma}^2 \alpha n_p^{\text{eff}}}{8} \left[\left(1 + \frac{\kappa^2}{4E^2} \right) \ln \left(1 + \frac{4E^2}{\kappa^2} \right) - 1 \right], \quad (2.1)$$

where α is the electromagnetic fine-structure constant, n_p^{eff} the effective number of targets, E the photon energy, and κ an appropriate screening scale which accounts for the finite range of the electric field of the charged particles in the stellar medium. This rate had been derived

Then, reduced Primakoff rate (taking into consideration all the assumptions about proton/electron degeneracy, reduction of the number of targets, reduction of proton mass):

$$\frac{d\dot{n}_a}{dE} = \frac{g_{a\gamma}^2 \xi^2 T^3 E^2}{8\pi^3 (e^{E/T} - 1)} \left[\left(1 + \frac{\xi^2 T^2}{E^2} \right) \ln(1 + E^2/\xi^2 T^2) - 1 \right], \quad (2.7)$$

where

$$\xi^2 = \frac{\kappa^2}{4T^2}. \quad (2.8)$$

Then, integrate it over volume of the star to obtain the total number of ALPs (assumed 50 km, so that the accounted EOS holds

PRIMAKOFF RATE (CONT.)

And, the final curve can be fit by...

An excellent fit to the total production rate is provided by the following expression [32], also widely used in SN neutrino studies,

$$\frac{d\dot{N}_a}{dE} = C \left(\frac{E}{E_0} \right)^\beta e^{-(\beta+1)E/E_0} . \quad (2.11)$$

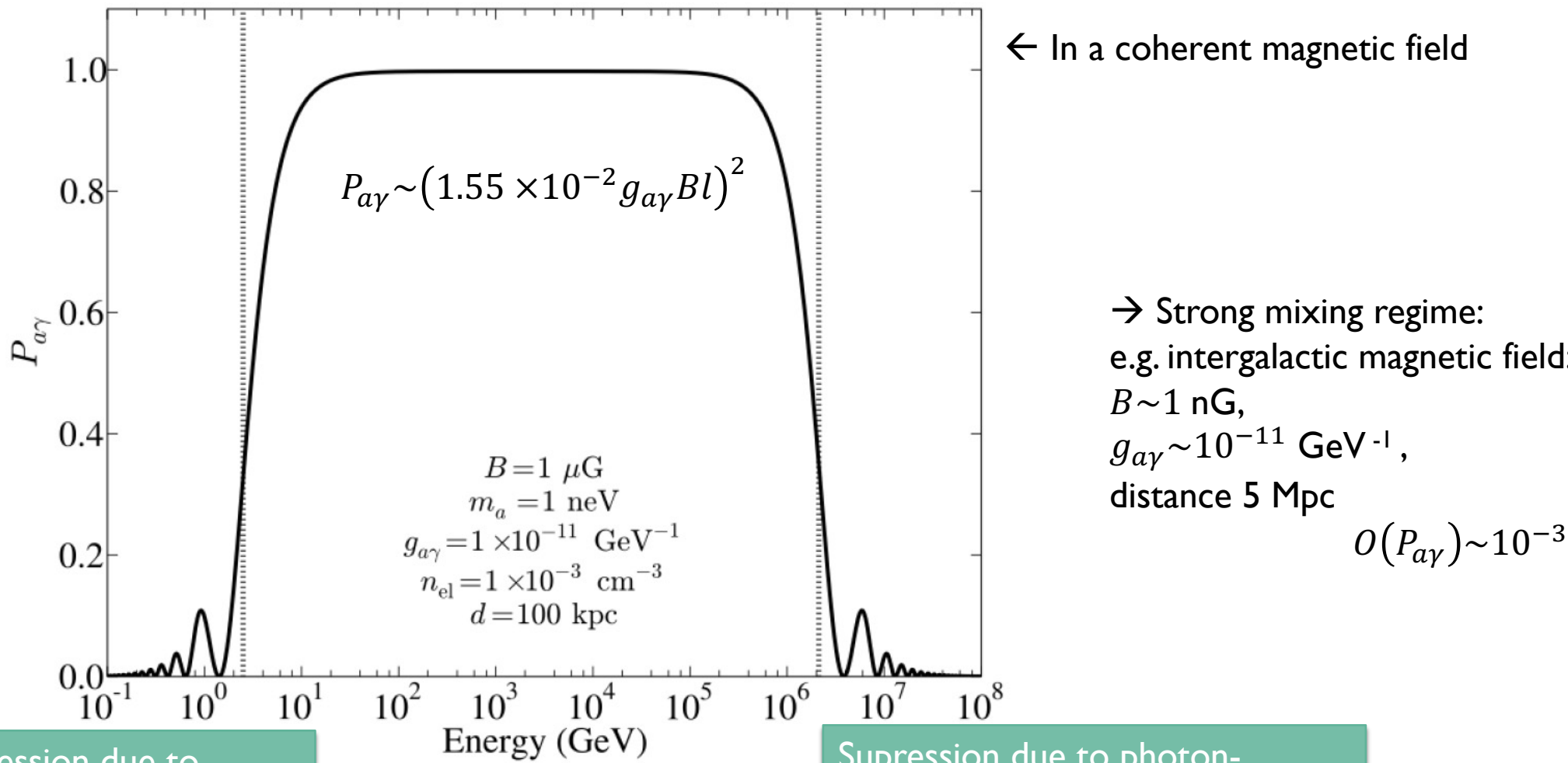
Here C is a normalization constant while the fit parameter E_0 coincides with the average energy $\langle E_a \rangle = E_0$. Numerically, we find $C = 1.03 \times 10^{52} \text{ MeV}^{-1} \text{ s}^{-1}$, $E_0 = 105.6 \text{ MeV}$, $\beta = 2.145$ for the curve corresponding to $t = 1 \text{ s}$ shown in Fig. 4. Similarly, we document for future use

Now, if we are interested in the differential ALP flux per unit energy at Earth, since the emission is necessarily isotropic in our model, we should simply consider

$$\frac{d\Phi_a}{dE} = \frac{1}{4\pi d^2} \frac{d\dot{N}_a}{dE} , \quad (2.12)$$

with d the distance to the supernova, which is 50 kpc in our case ($1 \text{ kpc} = 3.086 \times 10^{21} \text{ cm}$).

CONVERSION PROBABILITY VS ENERGY

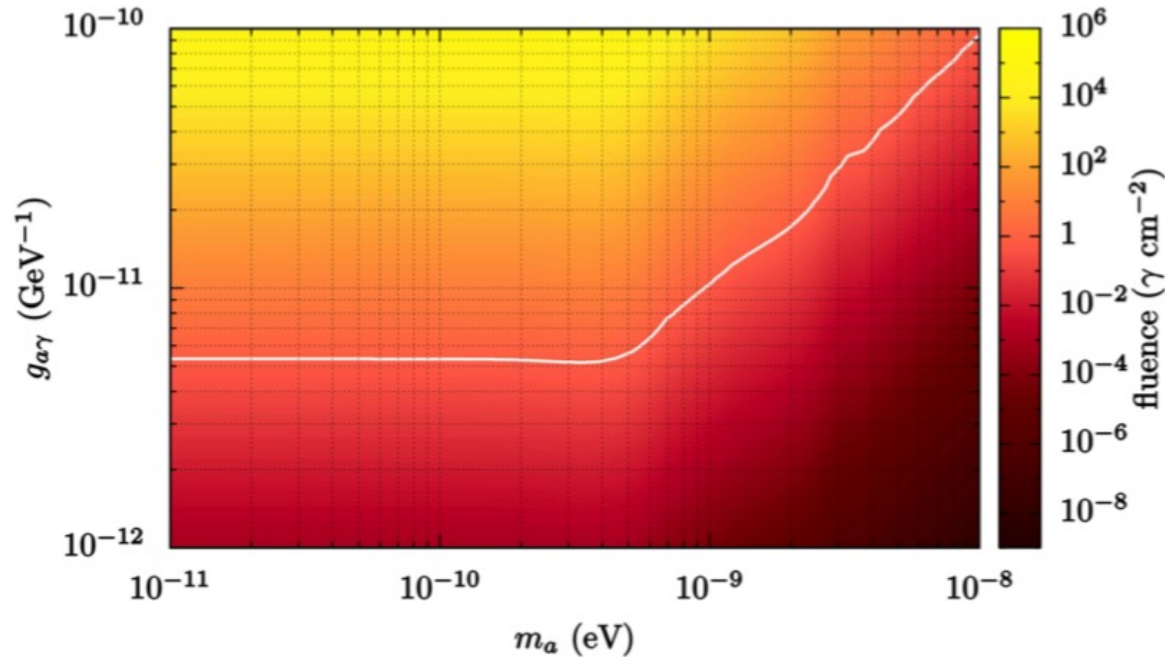


Supression due to
momentum mismatch
because of non-zero
ALP mass.

Supression due to photon-
photon dispersion with external
magnetic field and background
radiation fields (CMB)

[Dobrynina et al. 2015]

SN1987A



SN1987A fluence for a given coupling rate and the ALP mass. Stable upper bound: $g_{a\gamma} = 5.3 \times 10^{-12} \text{ GeV}^{-1}$ and $m_a = 4.4 \times 10^{-10} \text{ eV}$.

WILKS' THEOREM

$$D = -2 \ln \left(\frac{\text{likelihood for null model}}{\text{likelihood for alternative model}} \right)$$

- For large N_{tot} we can apply Wilks theorem and assume that the background distribution follows a χ_1^2 distribution.

$$p - \text{value} = \int_{\lambda_{\text{obs}}}^{\infty} dx \chi_k^2(x) = 1 - \text{erf}(\sqrt{\lambda_{\text{obs}}/2})$$

BACK-UP: OPTICAL LIGHTCURVES & EXPLOSION DETERMINATION

